symmetry

IMPACT FACTOR 2.7

CITESCORE 4.9

Article

Asymmetric Dark Matter in Baryon Asymmetrical Universe

Vitaly A. Beylin, Maxim Yu. Khlopov and Danila O. Sopin

MDPI

https://doi.org/10.3390/sym16030311

symmetry

MDPI

Article

Asymmetric Dark Matter in Baryon Asymmetrical Universe

Vitaly A. Beylin [1], Maxim Yu. Khlopov [1,2,3,*] and Danila O. Sopin [2,*]

[1] Virtual Institute of Astroparticle Physics, 75018 Paris, France; vitbeylin@gmail.com
[2] Institute of Nuclear Physics and Technology, National Research Nuclear University "MEPHI", 31 Kashirskoe Chaussee, 115409 Moscow, Russia
[3] Research Institute of Physics, Southern Federal University, Stachki 194, 344090 Rostov on Don, Russia
* Correspondence: khlopov@apc.in2p3.fr (M.Y.K.); sopindo@mail.ru (D.O.S.)

Abstract: New heavy particles with electroweak charges arise in extensions of the standard model. They should take part in sphaleron transitions in the early Universe, which balance baryon asymmetry with the excess of new charged particles. If electrically charged with charge $-2n$, they bind with n nuclei of primordial helium in dark atoms of dark matter. This makes it possible to find the ratio of densities of asymmetric dark matter and baryonic matter. Examples of the model with new, successive, and stable generation of quarks and leptons and the minimal walking technicolor model are considered.

Keywords: cosmoparticle physics; walking technicolor; stable multiple charged particles; sphaleron transitions; baryon asymmetry; new stable quarks; dark matter; dark atoms

1. Introduction

The modern cosmological paradigm assumes the presence in the Universe of a significant amount of dark matter (DM). The behavior of galaxies, gravitational lensing, the anisotropy of the cosmic microwave background, and other astrophysical observations confirm its existence, but the nature, dynamic characteristics, and possible observable manifestations of DM remain unknown, despite the many options for extending the standard model (SM) proposed to explain or predict them. The need to extend group of SM's gauge symmetry is due to the fact that, in the SM, there are no particles that could play the role of DM.

There are variety of ways to solve this problem in models describing physics beyond the SM (see [1,2]). In this article, we discuss two possible extensions: a model with a new sequential stable fourth generation [3–7] and a minimal walking technicolor (WTC) model [8–14]. Both models assume the existence of additional superheavy fermions with new gauge interaction. However, these models differ not only in the group of symmetry but also in the Higgs boson nature. While in WTC model, a single doublet describes the composite particle, in the model with a fourth generation, an additional heavy Higgs doublet is needed.

The topology of the electroweak gauge group $SU(2)$ leads to an existing of set of different vacua. The saddle point on the top of the potential barrier corresponds to the nontrivial solution of the field equations; this unstable solution is called "sphaleron". At high temperatures in the early Universe, it is possible to transit from one topological vacuum to another closest one via the sphaleron process changing the Chern–Simons number via unity. In such transitions, the laws of baryon and lepton numbers' conservation should be violated. This enables one to balance baryon asymmetry and the excess of dark matter particles over the corresponding antiparticles.

Because the potential barrier is high enough ($E_{Sph} \approx 9.1$ TeV), sphaleron transitions have not yet been observed. Using the data from collider experiments and cosmic rays observations [15,16], only the limits on the sphaleron rate can be set. Theoretical consideration shows that the rate of this process strongly depends on temperature (see review [17]).

Citation: Beylin, V.A.; Khlopov, M.Y.; Sopin, D.O. Asymmetric Dark Matter in Baryon Asymmetrical Universe. *Symmetry* **2024**, *16*, 311. https://doi.org/10.3390/sym16030311

Academic Editor: Eduardo Guendelman

Received: 31 January 2024
Revised: 23 February 2024
Accepted: 4 March 2024
Published: 6 March 2024

In Section 2, our thermodynamics approach is described. It was used to consider the model with new successive stable generation (Section 3) and the minimal WTC model (Section 4). A short review on the study of the sphaleron transitions rate is presented in Section 5. The results of numerical analyses are briefly discussed in the Conclusions.

2. Thermodynamic Approach

The thermodynamic approach to researching the cosmological consequences of sphaleron transitions was introduced in [18]. It has been developed and adopted for extensions of the standard model in [12–14]. This approach allows one to find the ratio of number densities for particles and then to consider the dependence of the energy densities on the parameters of the model.

If particles are in thermal equilibrium, the density of the baryon number can be defined as

$$B = \frac{6}{gT^2}(n_b - n_{\bar{b}}) = \frac{1}{3}\,T\,\sum \frac{\mu}{T}\,\sigma\left(\frac{m}{T}\right), \tag{1}$$

where the Taylor expansion is used for the distributions of baryons n_b and antibaryons $n_{\bar{b}}$. g, μ, and m represent the degrees of freedom, chemical potential, and the mass of a particular particle, respectively. The factor $\frac{1}{3}$ describes the baryon number of a single quark. Also, the weight function for a massive particle σ is

$$\sigma(z) = \begin{cases} \frac{6}{4\pi^2}\int_0^\infty dx\; x^2 \cosh^{-2}\left(\frac{1}{2}\sqrt{x^2+z^2}\right), & \text{for fermion;} \\ \frac{6}{4\pi^2}\int_0^\infty dx\; x^2 \sinh^{-2}\left(\frac{1}{2}\sqrt{x^2+z^2}\right), & \text{for boson.} \end{cases} \tag{2}$$

The lepton number density as well as the densities of charges are defined similarly.

As follows from the presented definition, the sign of the density is determined by the signs of chemical potentials. So, the sign is positive for particles and negative for antiparticles.

The chemical potentials should be introduced for each left/right particle. However, their number is reduced by electroweak conditions

$$\mu_{iR} = \mu_{iL} \pm \mu_0, \tag{3}$$

$$\mu_i = \mu_j + \mu_W, \tag{4}$$

where the particles "i" and "j" are the components of the weak doublet, μ_W is the chemical potential of the W^- boson, and μ_0 corresponds to the Higgs boson.

In both considered models, the new fermions are separated from the standard ones by the new charges. It makes the lightest particles stable and allows the formation of long-living bound states, which are generally calls "dark atoms". Also, the additional densities should be introduced. The densities of the fourth baryon and fourth lepton numbers (FB and FL) and the density of the y-charge Y are used in the fourth-generation model, and the densities of the technibaryon and technilepton numbers (TB and TL) are used in the WTC model.

The temperature T in Equation (1) is the sphaleron freezing-out temperature, which is assumed to be ∼200 GeV [19]. The exact value of this parameter depends on the rate of the sphaleron transitions, but its calculation is difficult (see Section 5). Following [12–14], we further use the range $T = 150$–250 GeV. So, for most particles of the standard model, the ratio $\frac{m}{T} \ll 1$, so $\sigma_f \approx 1$ (for fermions), and $\sigma_b \approx 2$ (for bosons). The only exception is quark t.

The system of equations depends on the ratio of the sphaleron freezing-out temperature T and the electroweak phase transition (EWPT) temperature T_c. If $T > T_c$; then, the condition of isospin neutrality $I_3 = 0$ could be used. But, in other cases, $T < T_c$, so the chemical potential of the Higgs boson must turn to zero $\mu_0 = 0$ because of vacuum condensation.

Considering the extensions of the standard model, it is natural to assume that the new particles have similar masses. In fact, the most significant results are obtained with

the approximation of equal masses. The study of deviations from this simplified case is difficult, since the masses of particles are included in the system of equations as arguments of weight functions. Therefore, we propose considering parametrization:

$$d_i = \sigma\left(\frac{m_i}{T}\right) - \sigma\left(\frac{m}{T_*}\right), \tag{5}$$

where m and T_* have values selected for convenience reasons; T is the sphaleron freezing-out temperature. The d_i parameters should vary in limits $[-\sigma\left(\frac{m}{T_*}\right); 0]$ and describe the values of "i"-particle's mass $[m; +\infty]$.

3. New, Successive, Stable Generation

New, successive, and stable generation [3,4,7] arises in heterotic string models. The additional fermions (two quarks U and D and two leptons N and E) are assumed to be superheavy: $m_U, m_D, m_E \sim 1\,\text{TeV}$, $m_U < m_D, m_E$ and $m_N \sim 50\,\text{GeV}$. These particles not only have standard gauge charges but also a new one y, which is the result of additional $U(1)$ symmetry. The main properties of successive generation are presented in Table 1.

Table 1. Properties of fourth-generation quarks.

Particle	Mass	Charge q	Charge y	New Lepton Number	New Baryon Number
U	~1 TeV	$\frac{2}{3}$	$-\frac{1}{3}$	0	$\frac{1}{3}$
D	~1 TeV	$-\frac{1}{3}$	$-\frac{1}{3}$	0	$\frac{1}{3}$
E	~1 TeV	-1	1	1	0
N	~50 GeV	0	1	1	0

To explain the high masses of the fourth-generation quarks and leptons, a second Higgs doublet is needed. So, the chemical potentials of the new particles should fulfill the following conditions:

$$\mu_{iR} = \mu_{iL} \pm \mu_{H_0}, \tag{6}$$

$$\mu_W = \mu_{H_0} + \mu_{H^-}, \tag{7}$$

$$\mu_i = \mu_j + \mu_W, \tag{8}$$

where μ_{H_0} and μ_{H^-} correspond to a heavy Higgs doublet. These equations were not taken into account in the previous study [5].

However, heavy neutrino is assumed to be much lighter than other particles of the fourth generation. This helps to avoid contradictions with precision measurements of SM parameters. Indeed, if the mass of the fourth neutrino is $\frac{M_Z}{2} < m_N < M_Z$, the radiation corrections are compensated for using Peskin–Tackeuchi parameters [4,6].

The electric charges of the new leptons and quarks are introduced by analogy with the charges of the standard generations. But, the values of y charges are determined from the condition of the reduction in $Z - \gamma - y$ and $Z - y - y$ anomalies (Z and γ are the standard neutral weak boson and photon; y is a new gauge boson) [7]. All standard model particles belong to the trivial representation of the new $U(1)$ group, so $y_{SM} = 0$.

The bound state $(\bar{U}\bar{U}\bar{U}\bar{N})^{--}He^{++}$—antineutrino-O-helium or ANO-helium—is stable because of y-charge conservation. It is a dark matter particle candidate. The cosmological consequences and the evolution in the early Universe were also considered in [3].

The chemical potentials of the new particles are introduced now as $\mu_{UL/R}$, $\mu_{DL/R}$, $\mu_{EL/R}$, and $\mu_{NL/R}$ for left-/right-handed fermions, respectively. In this way, the system of equations can be written out:

$$B = \frac{1}{3}\cdot 3\cdot(2+\sigma_t)(\mu_{uL}+\mu_{uR}) + \frac{1}{3}\cdot 3\cdot 3\cdot(\mu_{dL}+\mu_{dR}) = \\ = (10+2\sigma_t)\mu_{uL} + 6\mu_W, \tag{9}$$

$$L = \sum_i(\mu_{\nu_i L}+\mu_{\nu_i R}+\mu_{iL}+\mu_{iR}) = \\ = 4\mu + 6\mu_W. \tag{10}$$

The y-charge conservation law leads to the separation of standard baryon and lepton numbers and similar numbers of fourth-generation particles. So, the forth baryon number density FB and the forth lepton number density FL are defined as

$$FB = \frac{1}{3}\cdot 3\cdot\sigma_U(\mu_{UL}+\mu_{UR}) + \frac{1}{3}\cdot 3\cdot\sigma_D(\mu_{DL}+\mu_{DR}) = \\ = 2(\sigma_U+\sigma_D)\mu_{UL} + 2\sigma_D\mu_W + (\sigma_U-\sigma_D)\mu_{H^0}, \tag{11}$$

$$FL = \sigma_E(\mu_{EL}+\mu_{ER}) + \sigma_N(\mu_{NL}+\mu_{NR}) = \\ = 2(\sigma_N+\sigma_E)\mu_{NL} + 2\sigma_E\mu_W + (\sigma_N-\sigma_E)\mu_{H^0}. \tag{12}$$

The conditions of electro- and y-neutrality are

$$Q = 0 = \frac{2}{3}\cdot 3\cdot(2+\sigma_t)(\mu_{uL}+\mu_{uR}) - \frac{1}{3}\cdot 3\cdot 3\cdot(\mu_{dL}+\mu_{dR}) + \\ + \frac{2}{3}\cdot 3\cdot\sigma_U(\mu_{UL}+\mu_{UR}) - \frac{1}{3}\cdot\sigma_D(\mu_{DL}+\mu_{DR}) - \\ - 3(\mu_{eL}+\mu_{eR}) - \sigma_E(\mu_{EL}+\mu_{ER}) - 4\mu_W - 2\mu_- - 2\mu_{H^-}, \tag{13}$$

$$Y = 0 = -\frac{1}{3}\cdot 3\cdot\sigma_U(\mu_{UL}+\mu_{UR}) - \frac{1}{3}\cdot 3\cdot\sigma_D(\mu_{DL}+\mu_{DR}) + \\ + \sigma_E(\mu_{EL}+\mu_{ER}) + \sigma_N(\mu_{NL}+\mu_{NR}). \tag{14}$$

Before the EWPT, the condition of isospin neutrality can be used in the form

$$I_3 = 0 = \frac{1}{2}\cdot 3\cdot 3\cdot(\mu_{uL}-\mu_{DL}) + \frac{1}{2}\cdot 3\cdot(\mu_{\nu_i L}-\mu_{eL}) - 4\mu_W - (\mu_0+\mu_-) + \\ + \frac{1}{2}\cdot 3\cdot(\sigma_U\mu_{UL}-\sigma_D\mu_{DL}) + \frac{1}{2}(\sigma_N\mu_{NL}-\sigma_E\mu_{EL}) - (\mu_{H^0}+\mu_{H^-}). \tag{15}$$

Finally, the sphaleron transitions are described by the following equation:

$$3(\mu_{uL}+2\mu_{dL}) + \mu + (\mu_{UL}+2\mu_{DL}) + \mu_{NL} = 0. \tag{16}$$

In both cases (before and after the EWPT), the solution of this system of equations has the structure

$$\frac{\Omega_{DM}}{\Omega_b} = \frac{3m_U}{m_p}\left|\frac{FB}{B}\right|, \tag{17}$$

$$\frac{FB}{B} = -\alpha\left(\frac{L}{B}+\beta\right), \tag{18}$$

where the contribution of the fourth neutrino to the density is assumed to be negligible because of the mass of this particle. The functions α and β are dependent on the masses and sphaleron freezing-out temperature. The ratio $\frac{L}{B}$ is the free parameter that generally can be varied within infinite limits.

3.1. Before The Electroweak Phase Transition

Before the EWPT, the solution of the system of equations in the approximation of equal masses $m_U = m_D = m_E$ has the form (17), (18), where

$$\begin{aligned} \alpha &= \frac{\sigma_U(3\sigma_U^2 + (5\sigma_N + 24)\sigma_U + 24\sigma_N)}{16\sigma_U^2 + 136\sigma_U + 72}, \\ \beta &= 3. \end{aligned} \tag{19}$$

Both functions are positive for all possible values of weight functions, so the condition

$$\frac{L}{B} > -\beta = -3 \tag{20}$$

should be fulfilled to generate an excess of $\bar{U}\bar{U}\bar{U}$.

Because of $\alpha \sim \sigma_U$, the density ratio should decrease exponentially. Its dependence on the mass of heavy particles and the sphaleron freezing-out temperature is presented in Figure 1. The observed value of the $\frac{\Omega_{DM}}{\Omega_b}$ ratio [20] can be explained.

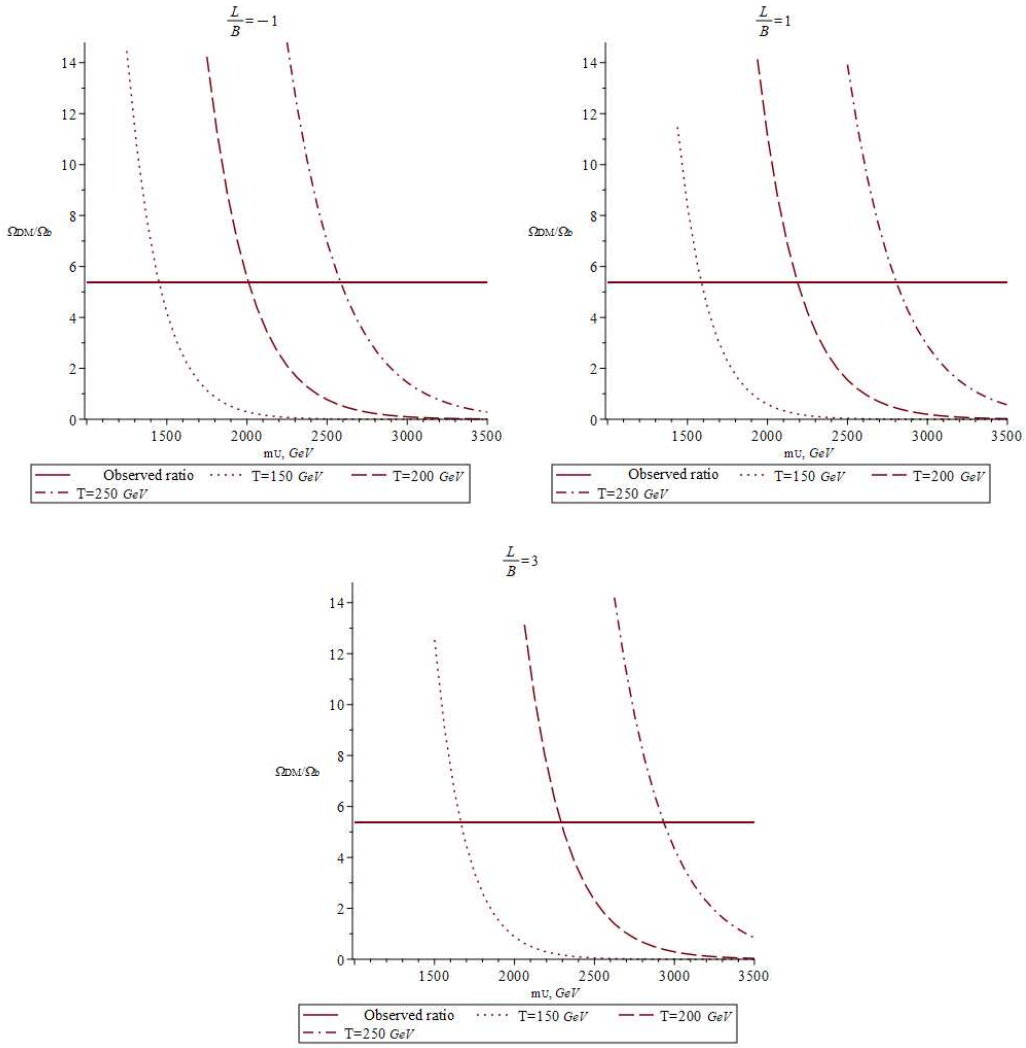

Figure 1. Density ratio $\frac{\Omega_{DM}}{\Omega_b}$ as a function of total mass and sphaleron freezing-out temperature.

The predicted mass interval increases linearly with the growth in the $\frac{L}{B}$ ratio's value. But, the overabundance of leptons should have an effect on nucleosynthesis; therefore,

$\frac{L}{B} < 10^7 - 10^8$ [21]. So, the upper limits on total mass can be found: $m_U < 9$ TeV, which means that $m_{ANO\text{-}He} < 27$ TeV.

Also, using Equation (18), it can be found that

$$B + L = -2B - \frac{8\left(2\sigma_U^2 + (2\sigma_N + 15)\sigma_U - 9\sigma_N\right)}{\sigma_U(3\sigma_U^2 + (5\sigma_N + 24)\sigma_U + 24\sigma_N)}FB, \tag{21}$$

$$B - L = 4B + \frac{8\left(2\sigma_U^2 + (2\sigma_N + 15)\sigma_U - 9\sigma_N\right)}{\sigma_U(3\sigma_U^2 + (5\sigma_N + 24)\sigma_U + 24\sigma_N)}FB, \tag{22}$$

where the factor before FB can be varied within $[4; +\infty)$. If the primordial Universe was baryon-symmetric, then $B - L = 0$. Since the $B - L$ difference conserves sphaleron transitions in the absence of an additional baryon number violating the processes, stricter limits on the total mass can be found for this special case: $m \sim (1600; 2700)$ GeV, which means $m_{ANO\text{-}He} \sim (4800; 8100)$ GeV for freezing-out temperature $T = (150; 250)$ GeV.

If masses of heavy particles are not equal, one can introduce

$$d, e = \sigma\left(\frac{m_{D,E}}{T_*}\right) - \sigma\left(\frac{m_U}{T}\right), \tag{23}$$

where the average value of the reference argument can be used $\frac{m_U}{T} = \frac{2000}{200} = 10$. These new variables can be varied within $[-\sigma_U, 0]$.

Simple calculations show that the value of the ratio $\frac{\Omega_{DM}}{\Omega_b}$ almost does not depend on the mass of the heavy electron E but decreases with increasing D quark mass (see Figure 2). So, the total mass limits can be optionally weakened.

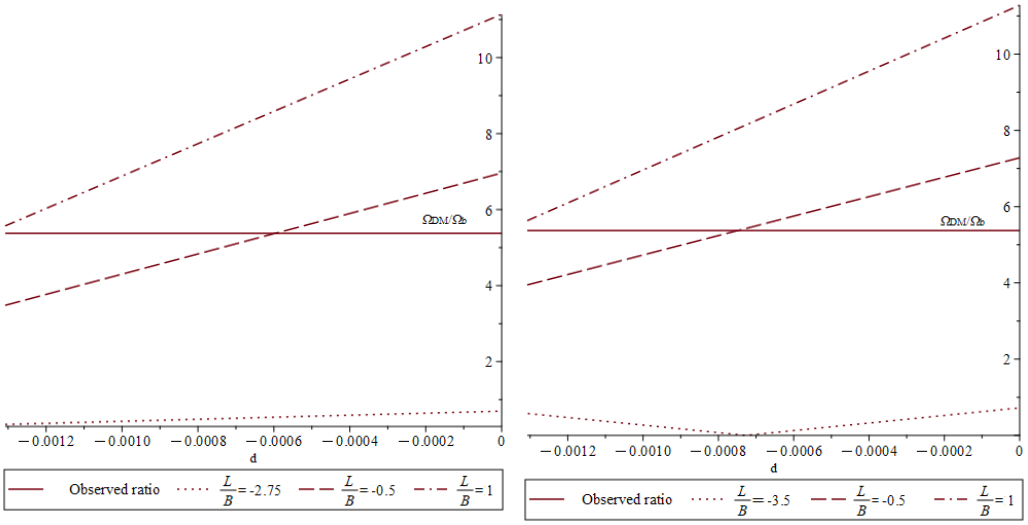

Figure 2. The ratio of densities $\frac{\Omega_{DM}}{\Omega_b}$ as a function of d before and after the EWPT (left and right panels, respectively).

3.2. After The Electroweak Phase Transition

The system of equations as well as its solution change if the sphaleron transitions freeze out after the EWPT. In this case, we obtain

$$\begin{aligned} \alpha &= \frac{\sigma_U\,(\sigma_t + 5)\,(5\sigma_N\sigma_U + 3\sigma_U^2 + 19\sigma_N + 21\sigma_U)}{(7\sigma_t + 89)\sigma_U^2 + ((25\sigma_t + 71)\sigma_N + 145\sigma_t + 455)\sigma_U + (87\sigma_t + 273)\sigma_N}, \\ \beta &= \frac{54\sigma_U^2 + (90\sigma_N + 32\sigma_t + 322)\sigma_U + (40\sigma_t + 326)\sigma_N}{(\sigma_t + 5)(5\sigma_N\sigma_U + 3\sigma_U^2 + 19\sigma_N + 21\sigma_U)}. \end{aligned} \tag{24}$$

The ratio of densities as a function of total mass is shown in Figure 3. Significant differences arise only in the parameter regions in which the overproduction of DM is predicted. So, the upper limit on the total mass coincides with what was obtained for the previous case: $m_U < 9\,\text{TeV}$ and $m_{ANO\text{-}He} < 27\,\text{TeV}$.

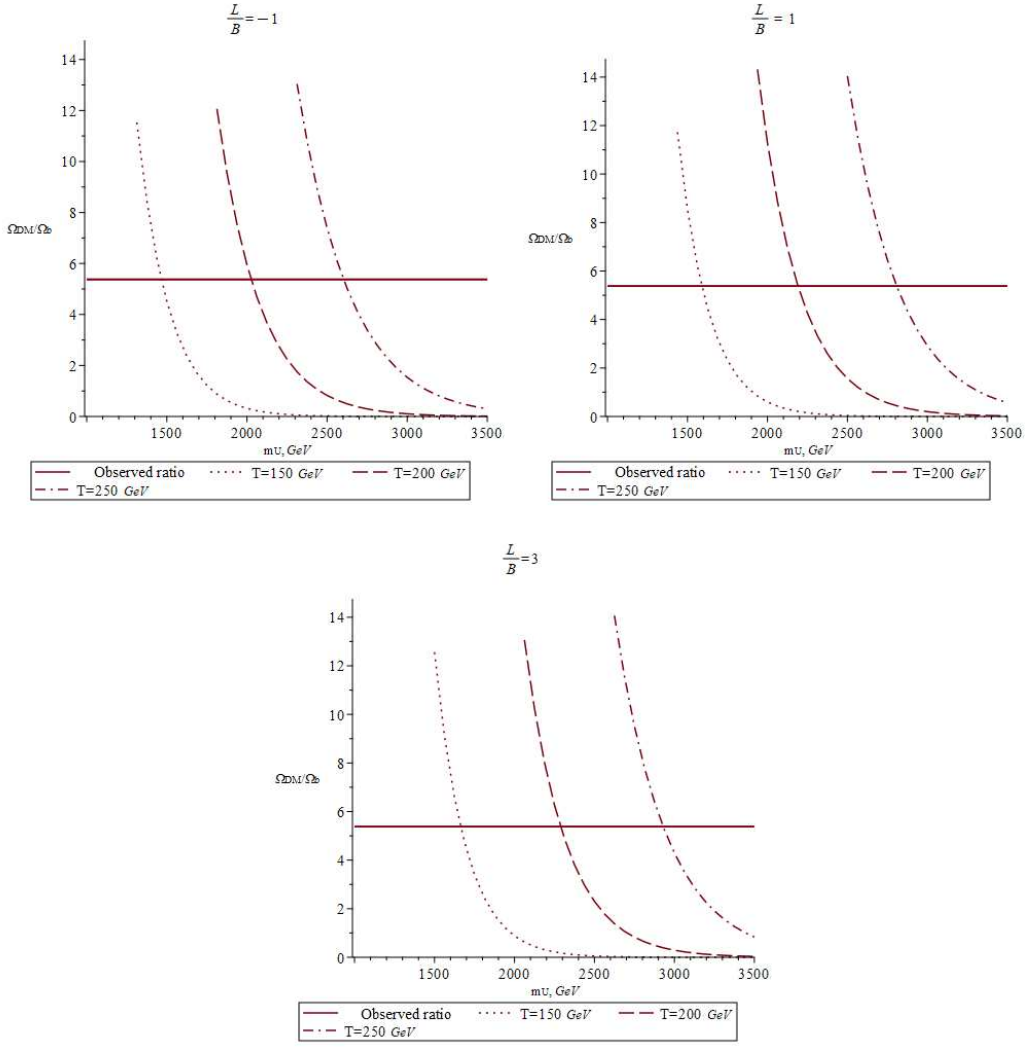

Figure 3. The ratio of densities as a function of total mass. Sphaleron transitions freeze out after the EWPT.

The function β now depends on the mass and freezing-out temperature; therefore, the minimal value of ratio $\frac{L}{B}$ can change in a narrow region $\sim (-3.15)$–(-3.24).

The equations similar to (21) and (22) are

$$B + L = -\frac{\sigma_t + 11}{\sigma_t + 5} B + \varkappa B - \lambda F B, \tag{25}$$

$$B - L = 3\,\frac{\sigma_t + 7}{\sigma_t + 5} B - \varkappa B + \lambda F B, \tag{26}$$

where coefficients $\varkappa$ and λ are the bulky functions of total mass and the sphaleron freezing-out temperature. In the case of a baryon-symmetric primordial Universe, it gives total mass limits of $m \sim (1500; 2800)$ GeV, which mean $m_{ANO\text{-}He} \sim (4500; 8400)$ GeV.

As in the previous case, the ratio of densities $\frac{\Omega_{DM}}{\Omega_b}$ is almost independent of the mass of heavy electrons E, but the dependence on D quark changes a bit. This is shown in Figure 2. If the value of parameter $\frac{L}{B}$ is high, then the behaviors of the functions are quite similar.

But, around the critical value, a line break occurs in this case after the EWPT. So, the ratio $\frac{m_i}{T}$ should be considered, not only the mass value m_i.

Also, the dependence of this ratio on the heavy neutrino's mass is negligible. Only if this mass is in the TeV scale would the value of the ratio decrease.

3.3. Discussion

The considered cases are quite similar despite changes in the systems of equations. The found limits on the masses of new particles can be combined as $m_{ANO\text{-}He} < 27\,\text{TeV}$ for the general case or $m_{ANO\text{-}He} \sim (4500; 8400)\,\text{GeV}$ for the baryon-symmetric primordial Universe. Particles with such masses can be reached at the LHC. The search should be similar to the one for long-lived particles from various SUSY scenarios (R-hadrons, bound color-singlet objects generated via the hadronization of gluino) [22–24].

It should be noted that the mass of the additional Higgs boson is not specified in this calculation. Its inclusion in Equations (13) and (15) leads to changes in the values of some numerical coefficients, but the general behavior of the ratios of densities and the resulting mass limits remain the same.

4. The Minimal Walking Technicolor Model

DM particle candidates in form of dark atoms also arise in the minimal walking technicolor model (WTC) [8–11]. New heavy fermions (U, D, and N, E) belong to the adjoined representation o the technicolor $SU(2)$ group. So, techniquarks U and D, in addition to electroweak charges, have a new one—technicolor. Technileptons N and E are introduced to eliminate anomalies.

The global symmetry of the model is spontaneously broken $SU(4) \to SO(4)$, which leads to the existence of nine Goldstone bosons. They correspond to the longitudinal components of massive bosons W and Z and technibaryons UU, UD, and DD with their antiparticles.

The arbitrary electric charges of the new particles are not fixed. To describe it, one can introduce the y parameter as follows [12–14]: $q = y + 1$, y, $y - 1$ and $\frac{1}{2}(-3y + 1)$, $\frac{1}{2}(-3y - 1)$ for UU, UD, DD and N, E correspondingly. Also, technibaryons form the electroweak triplet (UU,UD,DD) with isospin projections (1,0,−1). The left leptons belong to the doublet (N,E).

The lightest techniparticles are assumed to be stable. Therefore, the $(-2n)$-charged (anti)technibaryon UU^{-2n} and (anti)technileptons $(N/E)^{-2n}$ should form the heavy cores of X-helium dark atoms $X^{-2n}(He^{+2})_n$. The special case $y = 1$ has already been studied [12–14]. In this section, the cosmological consequences of the general case are considered.

According to the results of recent research on multicharged particles [25], the mass of techniparticles with multiple charges should be $m > 1\,\text{TeV}$. In this paper, it is also expected that $m_U < m_D$. The ratio of masses of technileptons cannot be set in general case. The type of the lightest lepton depends on the charge parameter y and is conditioned by the requirements of no-go theorem [26].

There are no changes in the definitions of the densities of standard baryon and lepton numbers. They are similar to (9), (10) and the ones that were used in [12–14,18]:

$$B = (10 + 2\sigma_t)\mu_{uL} + 6\mu_W, \tag{27}$$

$$L = 4\mu + 6\mu_W. \tag{28}$$

The densities of technibaryon and technilepton numbers are separate from those of the standard ones. They can be written out as

$$TB = \frac{2}{3}(\sigma_{UU}\mu_{UU} + \sigma_{UD}\mu_{UD} + \sigma_{DD}\mu_{DD}), \tag{29}$$

$$TL = \sigma_E(\mu_{EL} + \mu_{ER}) + \sigma_N(\mu_{NL} + \mu_{NR}), \tag{30}$$

where the chemical potentials of tehniparticles (μ_{UU}, μ_{UD}, μ_{DD} for technibaryons and $\mu_{NL/R}$, $\mu_{EL/R}$ for left/right technileptons) are introduced.

The electroneutrality equation takes into account the parameterization of the charges in heavy particles:

$$\begin{aligned} 0 =& \frac{2}{3}\cdot 3\cdot 3(\mu_{uL}+\mu_{uR}) - \frac{1}{3}\cdot 3\cdot 3(\mu_{dL}+\mu_{dR}) - \frac{1}{3}(\mu_{eL}+\mu_{eR}) + \\ &+ (y+1)\sigma_{UU}\mu_{UU} + y\sigma_{UD}\mu_{UD} + (y-1)\sigma_{DD}\mu_{DD} + \\ &+ \frac{-3y+1}{2}\sigma_N(\mu_{NL}+\mu_{NR}) + \frac{-3y-1}{2}\sigma_E(\mu_{EL}+\mu_{ER}) - 4\mu_W - 2\mu_m. \end{aligned} \tag{31}$$

The sphaleron equation and the condition of isospin projection neutrality (for case $T > T_c$) are similar to those in [12–14]:

$$3(\mu_{uL}+2\mu_{dL}) + \mu + \frac{1}{2}\mu_{UU} + \mu_{DD} + \mu_{NL} = 0, \tag{32}$$

$$\begin{aligned} 0 =& \frac{1}{2}\cdot 3\cdot 3\cdot(\mu_{uL}-\mu_{dL}) + \frac{1}{2}\cdot 3\cdot 3\cdot(\mu_{iL}-\mu_{eL}) + \\ &+ \sigma_{UU}\mu_{UU} - \sigma_{DD}\mu_{DD} + \frac{1}{2}\sigma_N\mu_{NL} - \frac{1}{2}\sigma_E\mu_{EL} - 4\mu_W - \mu_W. \end{aligned} \tag{33}$$

For the chemical potentials of the techniparticles, some conditions should be introduced. Following [12], the electroweak decay equations are

$$\begin{aligned} \mu_{UD} &= \mu_{UU} + \mu_W, \\ \mu_{DD} &= \mu_{UU} + 2\mu_W. \end{aligned} \tag{34}$$

The condition for the lightest technilepton is similar to the standard condition.

But, the value of the Higgs boson chemical potential is fixed in this study,

$$\mu_0 = 0 \tag{35}$$

and does not depends on the sphaleron freezing-out temperature. It is assumed in Equations (32) and (34) that the chemical potential of the bound state can be introduced as a sum of the potentials of its constituent parts. So, in the considered model, the Higgs boson, which is in the bound state $\frac{1}{\sqrt{2}}(U\bar{U} + D\bar{D})$, should be zero because the chemical potentials of the particle and antiparticle differ only in sign.

This is a significant change compared with that in previous studies [12–14]. If the sphaleron transitions freeze out before the EWPT, it adds one more equation to the system.

4.1. Before The Electroweak Phase Transition

If sphaleron transitions freeze out before the EWPT, the system of equations can be solved for two ratios of densities:

$$\frac{TB}{B} = -\frac{\sigma_{UU}(3y\sigma_E - 1)}{3y(\sigma_{UU} + 3\sigma_E)}\left(\frac{L}{B} + \frac{9y\sigma_E + 1}{3y\sigma_E - 1}\right), \tag{36}$$

$$\frac{TL}{B} = -\frac{\sigma_E(y\sigma_{UU} + 1)}{y(\sigma_{UU} + 3\sigma_E)}\left(\frac{L}{B} + \frac{3y\sigma_{UU} - 1}{y\sigma_{UU} + 1}\right), \tag{37}$$

where the assumption of equal masses $m_{UU} = m_{UD} = m_{DD}$ and $m_N = m_E$ is used. These solutions have a similar structure

$$\frac{TB}{B}, \frac{TL}{B} = -\alpha\left(\frac{L}{B} + \beta\right) \tag{38}$$

and can be combined in the ratio of densities of dark and baryonic matter

$$\frac{\Omega_{DM}}{\Omega_b} \approx \frac{\Omega_{UU}}{\Omega_b} + \frac{\Omega_L}{\Omega_b} = \frac{3m_{UU}}{2m_p}\left|\frac{TB}{B}\right| + \frac{3m_{N/E}}{m_p}\left|\frac{TL}{B}\right|. \tag{39}$$

One more approximation can be introduced to simplify the following consideration. The mass assumption $m_{N/E} = \frac{m_{UU}}{2}$ allows the suppression of the density of technibaryons. For high masses of new particles, the prefactors in Equations (36) and (37) are

$$\alpha_{TB} = \frac{\sigma_{UU}(3y\sigma_E - 1)}{3y(\sigma_{UU} + 3\sigma_E)} \sim \frac{\sigma_{UU}}{\sigma_E}, \tag{40}$$

$$\alpha_{TL} = \frac{\sigma_E(y\sigma_{UU} + 1)}{y(\sigma_{UU} + 3\sigma_E)} \sim \frac{\sigma_E}{\sigma_E} = 1, \tag{41}$$

where the ratio $\frac{\sigma_{UU}}{\sigma_E}$ decreases exponentially.

As functions of the charge parameter, both ratios of densities ($\frac{\Omega_{UU}}{\Omega_b}$ and $\frac{\Omega_L}{\Omega_b}$) have a hyperbolic form. This is shown in Figure 4. This dependence arises due to the condition on the Higgs boson chemical potential.

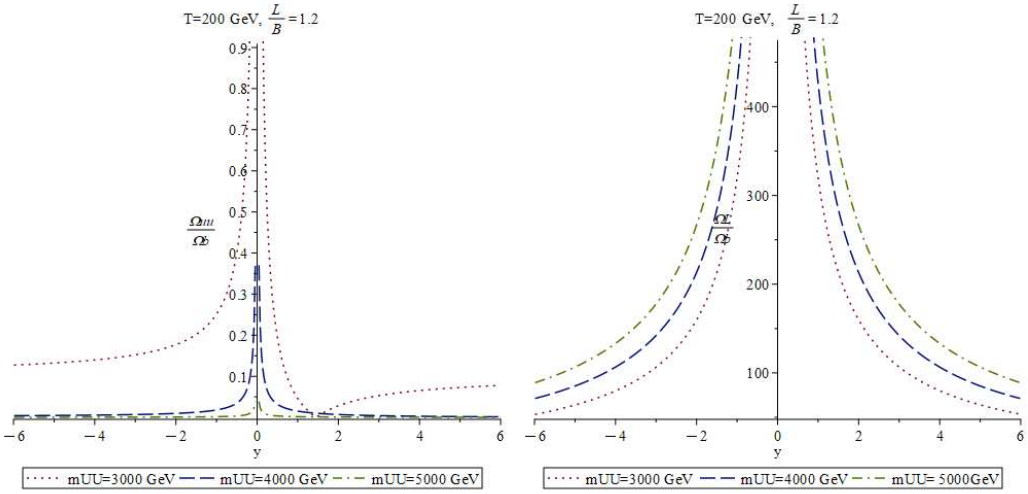

Figure 4. The ratios of densities as functions of charge parameter y.

The sign of the ratios of numbers can change because of factors $(3y\sigma_E - 1)$ and $(y\sigma_{UU} + 1)$ in Equations (36) and (37), respectively. As such, the possible composition of dark atoms depends on the model's parameters. The line break in the left panel in Figure 4 shows the values at which the excess of technibaryons transforms into an excess of antitechnibaryons. In Table 2, the "critical" values of masses at which this occurs are written out for several significant, particular cases.

If the value of the charge parameter is $y = 1$, the critical value of mass is too low. Indeed, it can be found that $\sigma_f^{\max}\left(\frac{m_f^{\min}}{T}\right) = \sigma_f\left(\frac{1000}{250}\right) \approx 0.167 < \frac{1}{3y} = \frac{1}{3}$. So, the considered effect cannot be observed in this case.

The density of the technilepton number should change its sign for negative values of charge parameter y. Let the bosonic weight function have the highest possible physical value $\sigma_b^{\max} = \sigma_b\left(\frac{2000}{250}\right) \approx 0.007$. So, the sign of the density changes at $y \approx -\frac{1}{\sigma_b^{\max}} \approx -138$. This value of the charge parameter seems unnatural.

The ratio $\frac{L}{B}$ varies within infinite limits; therefore, it also affects the physical picture significantly. In Figure 5, it is shown how the mass dependence of the ratio of densities changes for different values. The charge parameter value is fixed at $y = 3$. The ATLAS

experimental limit [25] is plotted with vertical green lines; the observed [20] value of the density ratio is represented by the horizontal line.

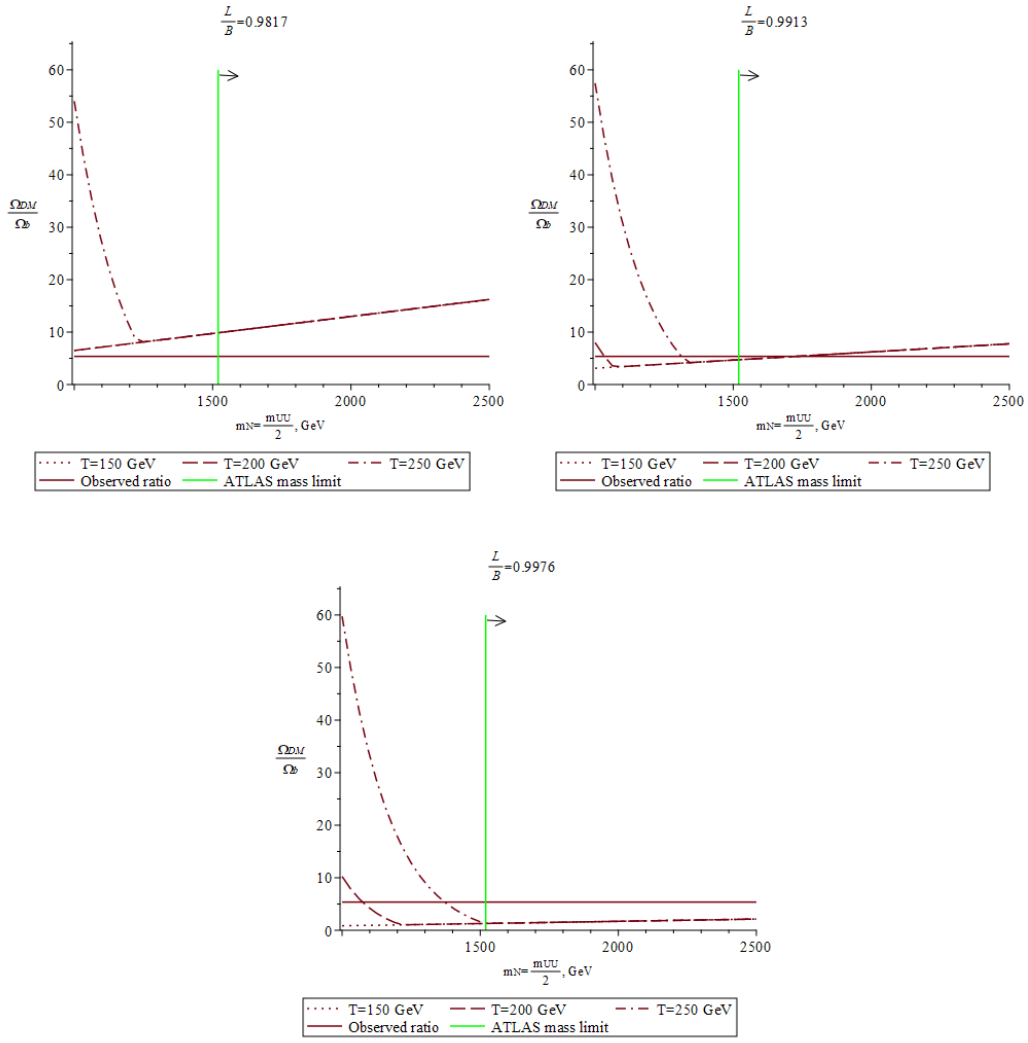

Figure 5. The dependence of the ratio of densities on total mass ($m_E = \frac{m_{UU}}{2}, y = 3$) for different values of $\frac{L}{B}$.

Table 2. The critical values of total mass in assumption $m = m_{N/E} = \frac{m_{UU}}{2}$.

y	$\sigma_f^{\text{crit}} = \frac{1}{3y}$	m^{crit}, GeV		
		$T_* = 250\,\text{GeV}$	$T_* = 200\,\text{GeV}$	$T_* = 150\,\text{GeV}$
3	$\frac{1}{9}$	≈ 1141	≈ 913	≈ 684
5	$\frac{1}{15}$	≈ 1311	≈ 1048	≈ 786

Equation (39) linearly depends on $\frac{L}{B}$, which leads to the danger of the overproduction of techniparticles. Actually, experimental constraints can be satisfied only in a narrow region of parameter values. This is shown in Figure 6. Grey areas are forbidden because of

(1) The overproduction of both types of techniparticles;
(2) The overproduction of technileptons;
(3) The overproduction of technibaryons;
(4) The overproduction of the anomalous isotopes, arising from an excess of positively charged techniparticles of both types.

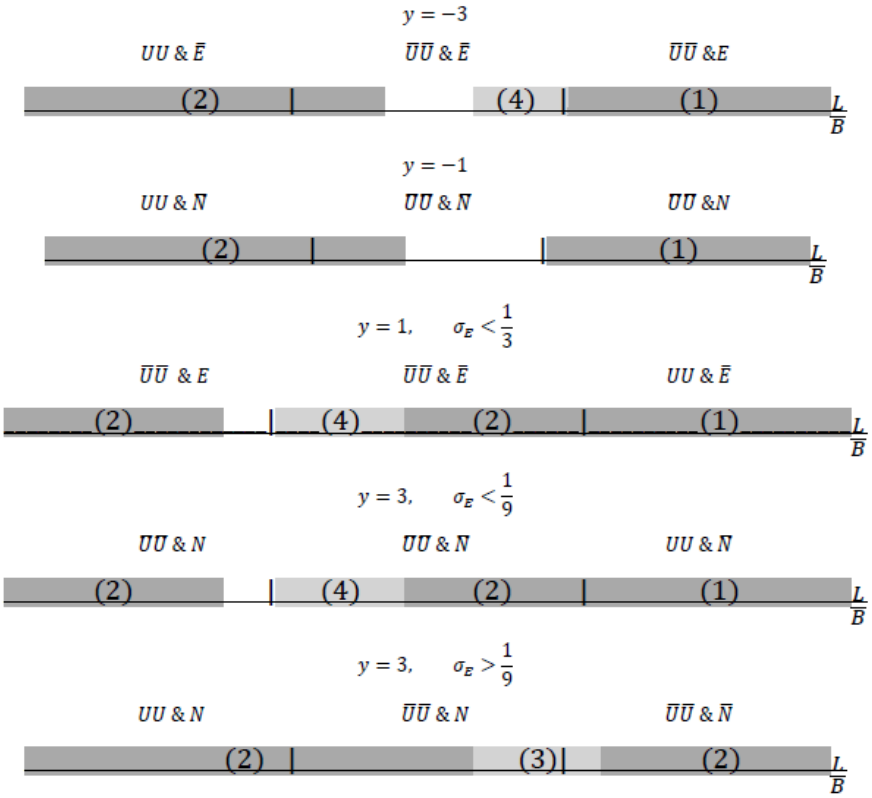

Figure 6. Allowed and forbidden parameter regions for small values of the charge parameter.

The white areas correspond to the allowed regions. They lie near the points (vertical lines in Figure 6) where the sign of the ratios of number densities changes due to the value of $\frac{L}{B}$.

The overproduction of techniparticles also occurs in the case of multicharged ($y \leq 3$) light ($m < m^{\text{crit}}$) particles. It gives the lower limits on masses.

The composition of a dark matter particle depends on the value of the charge parameter y. In the allowed area for

- $y > 0$, two forms of X-helium exist. DM mainly consists of technilepton dark atoms $(N/E)^{\frac{-3y\pm1}{2}}(^4He^{+2})_{\frac{-3y\pm1}{4}}$, but the exponentially suppressed density of technibaryons is provided by $(\bar{U}\bar{U})^{y+1}(^4He^{+2})_{\frac{y+1}{2}}$.
- The special case $y = -1$. There is only one form of dark atom—technileptonic O-helium $\bar{E}He$. Technibaryons form the WIMP $\bar{U}\bar{U}$, but its density is low due to suppression.
- $y < -1$, where technileptons and technibarions have electric charges of different signs. This leads to the existence of a more complex set of bound states. At the right boundary of the allowed area, the density of the hidden mass is provided by the WIMP-like state $(\bar{U}\bar{U})_m(\bar{N})_n$, where m and n fulfill the following equation:

$$-2m(y+1) - n(-3y \pm 1) = 0. \tag{42}$$

But, at the left boundary, two types of X-helium can also be found. Because the density of technileptons increases, dark atoms with technileptonic $\bar{N}^{-2r}$ and mixed $\bar{N}^{-2r}(\bar{U}\bar{U})^{+2s}$ cores can form.

This pattern remains if any another $m_{UU} \geq m_{N/E}$ mass assumption is used. But, the area's boundaries can change. The function

$$\begin{aligned} \Delta = \left| \frac{L}{B}\left(\frac{TB}{B}=0\right) - \frac{L}{B}\left(\frac{TL}{B}=0\right) \right| &= |\beta_{TB} - \beta_{TL}| \\ &\approx 4\left| \frac{y(\sigma_{UU}+3\sigma_E)}{(3y\sigma_E-1)(y\sigma_{UU}+1)} \right| \end{aligned} \tag{43}$$

can be used to estimate the allowed area's dynamics. Its value increases if the function's value grows and vice versa.

For example, in $m_{UU} = m_{N/E}$, the suppression of a technibaryon component of DM is almost removed. In Figure 7, the technibaryonic density ratio's dependencies on mass are plotted for different $\frac{L}{B}$ values, $T = 200\,\text{GeV}$. This is similar to the technileptonic function. Dark atoms with a technibaryonic core should play a significant role now; however, the danger of overproduction is greatly increased.

In both cases, $y > 0$ and $y < 0$, the removal of suppression leads to the formation of WIMPs. For negative values of the charge parameter, the description does not change at all. But, in the "positive" case, some of the anomalous isotopes transform into WIMPs in (4)-type areas.

In Figure 8, the general dependence of the ratios of densities on the mass difference $\Delta m = m_{UU} - m_{N/E}$ is presented. To avoid the overproduction of DM, in most cases, it is necessary to fine tune the parameters.

Also, it should be mentioned that the highest possible physical value of the bosonic weight function in the considered assumption is $\sigma_b^{\max} = \sigma_b\left(\frac{1000}{250}\right) \approx 0.171$. Therefore, the sign of the technilepton number can be changed by varying the particle mass at $y < -\frac{1}{\sigma_b^{\max}} \approx -5.8$. However, to fulfill the no-go theorem, one should consider the consequences of this effect for $y \leq -7$.

It can be seen from Figure 9 that there are no allowed regions for the parameters in the case where $y = -7$, $m_{UU} < m_{\text{crit}}$. The overproduction of techniparticles is observed for all values of $\frac{L}{B}$ ratio.

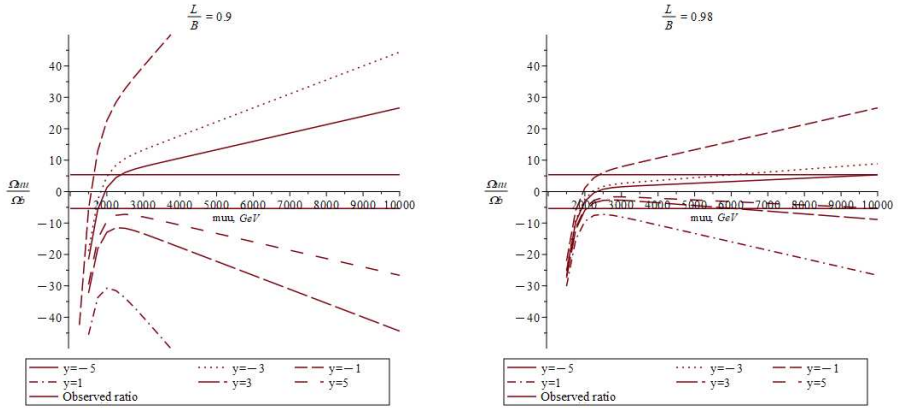

Figure 7. *Cont.*

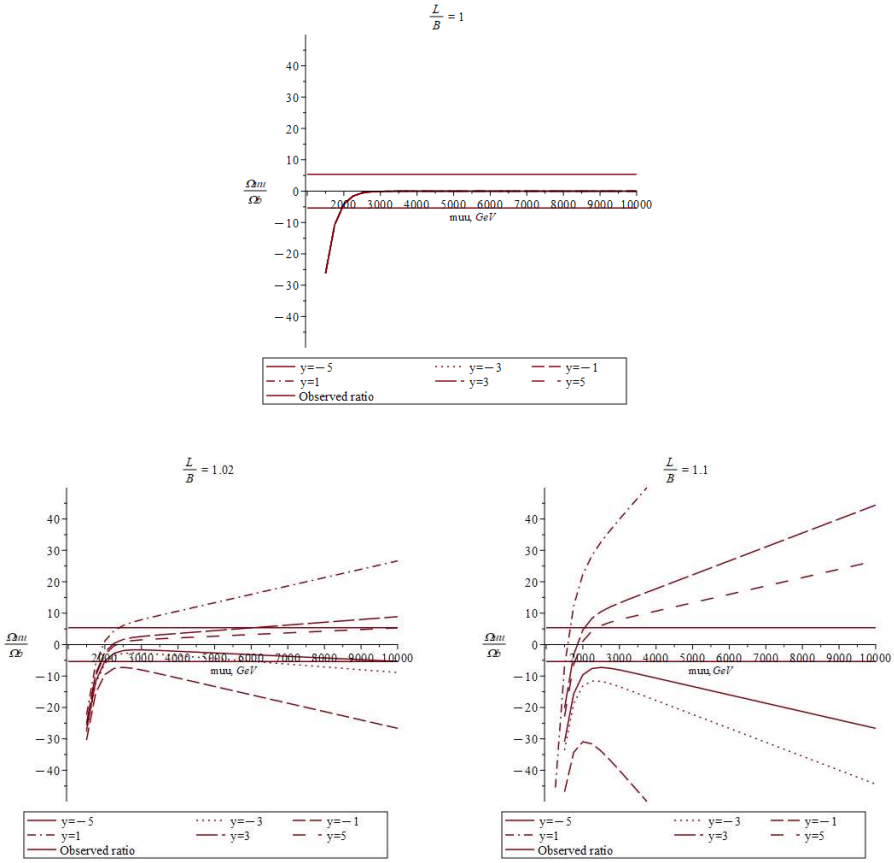

Figure 7. The ratio of technileptonic DM and baryonic matter as a mass function in assumption $m_{UU} = m_{N/E}$.

To estimate the dependence of the density ratios on the difference in mass, it is necessary to introduce the following parameterization (5):

$$\sigma_{N,E} = \sigma_f\left(\frac{m}{T}\right) + n, e, \tag{44}$$

$$\sigma_{UU} = \sigma_b\left(\frac{m}{T}\right) + 2u, \tag{45}$$

$$\sigma_{UD} = \sigma_b\left(\frac{m}{T}\right) + u + d, \tag{46}$$

$$\sigma_{DD} = \sigma_b\left(\frac{m}{T}\right) + 2d. \tag{47}$$

The reference argument of weight functions is $\frac{m}{T} = \frac{1500}{250}$.

The ratios of number densities as functions of these parameters are plotted in Figures 10 and 11 for $y = 3$, $\frac{L}{B} = 1$ and $\frac{L}{B} = 0.8$, respectively. The red dots indicate the values obtained in the approximation of equal masses ($m_N = m_E = m_{UU} = m_{UD} = m_{DD}$).

The high mass difference of techniparticles leads to the increase in the values of the ratios of number densities. In some cases (see "d–u" plots), the sign of the ratio of densities changes. So, the boundaries of allowed region strongly depends on these parameters.

It is also useful to consider the special case of the baryon-symmetric primordial Universe ($\frac{L}{B} = 1$). There is no suppression of the technibaryon component for any mass assumption:

$$\frac{TL}{TB} = 3\,\frac{\sigma_E}{\sigma_{UU}}\,\frac{y\left(\frac{L}{B}+3\right)\sigma_{UU}+\frac{L}{B}-1}{3y\left(\frac{L}{B}+3\right)\sigma_E-\frac{L}{B}+1} = 1. \tag{48}$$

And, the ratio of densities has a simple form:

$$\frac{\Omega_{DM}}{\Omega_b} = 6\,\frac{m_{UU}+2m_{N/E}}{m_p}\,\frac{\sigma_{UU}\sigma_E}{\sigma_{UU}+3\sigma_E}. \tag{49}$$

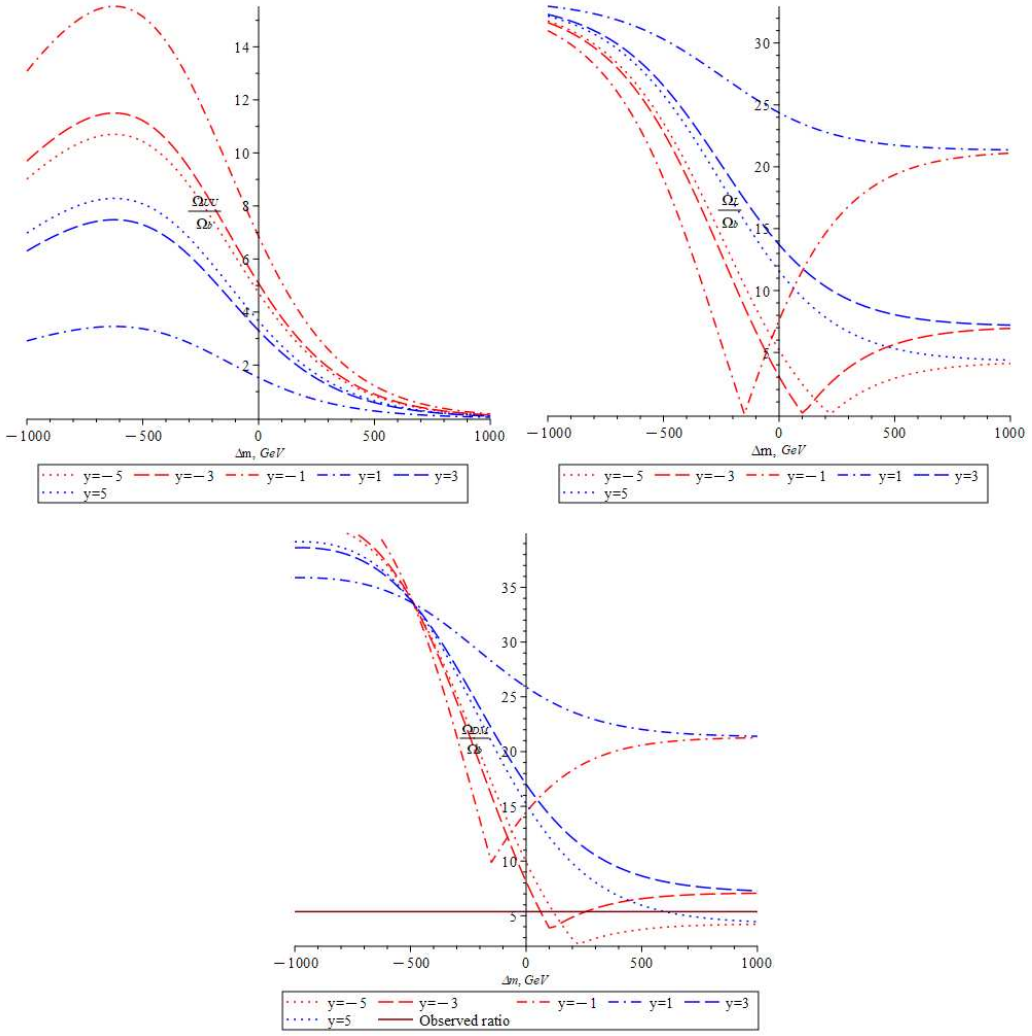

Figure 8. The general dependence of the ratios of densities on the mass difference $\Delta m = m_{UU} - m_E$.

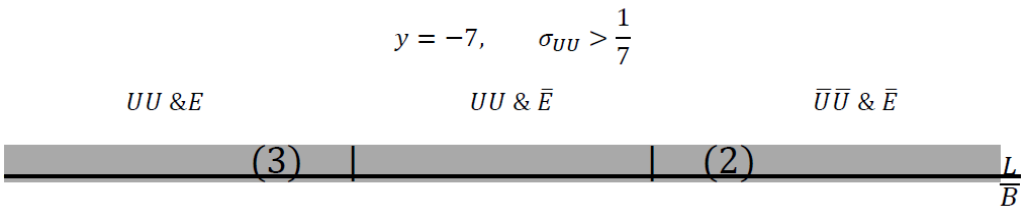

Figure 9. The forbidden parameter regions for $y = -7$ and $m_{UU} < m_{\text{crit}}$.

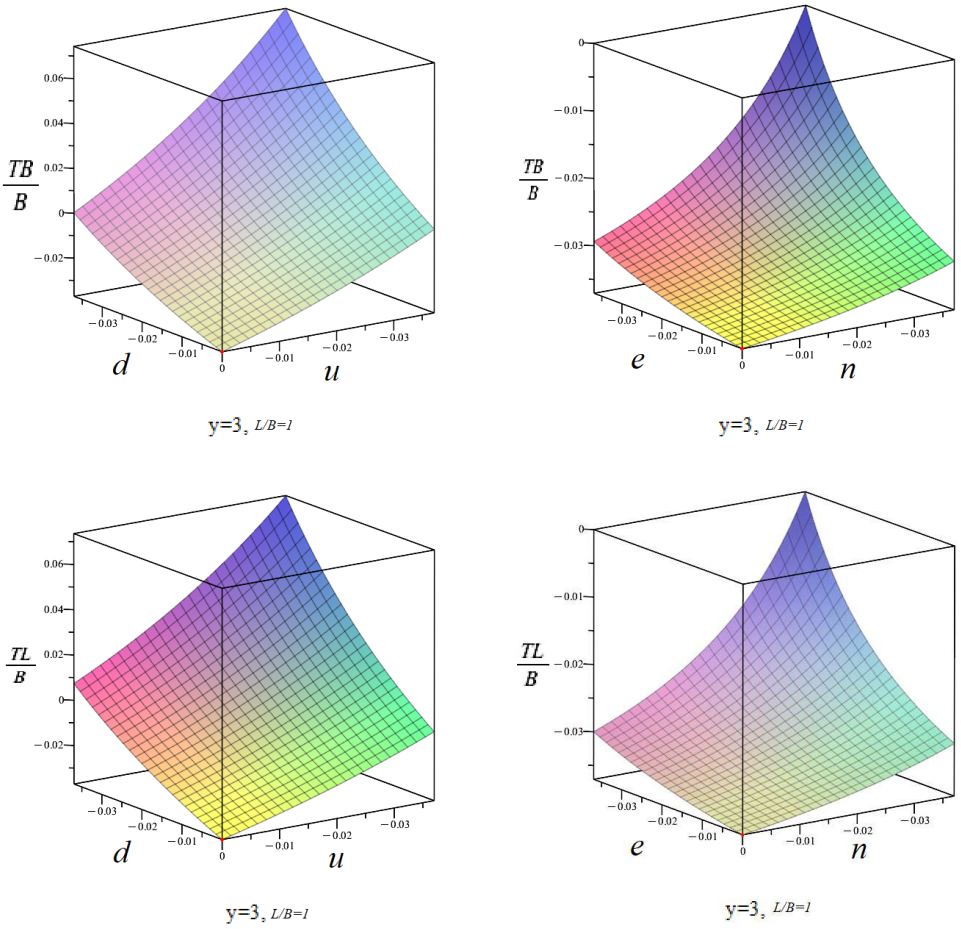

Figure 10. The ratio of number densities as a function of mass differences. Case $\frac{L}{B} = 1$.

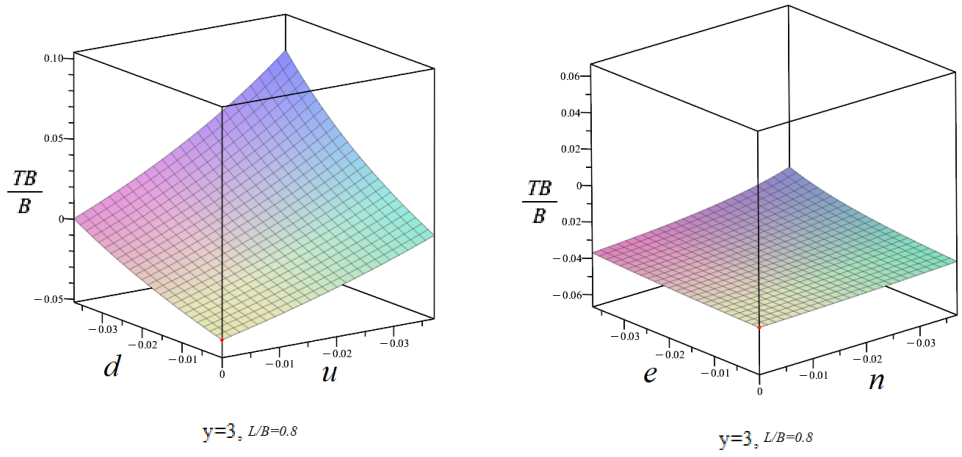

Figure 11. *Cont.*

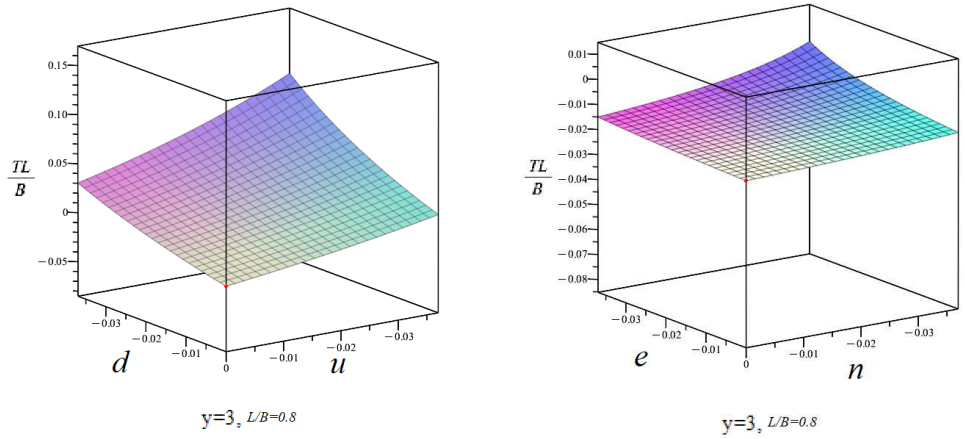

Figure 11. The ratio of number densities as a function of mass differences. Case $\frac{L}{B} = 0.8$.

In this case, dark matter consists of WIMP-like bound states. Therefore, this scenario can be classified as undesirable.

The equations

$$\begin{aligned} B - L &= 4\,B + \frac{(\sigma_{UU} + 3\sigma_E)y}{(y\sigma_{UU} + 1)\sigma_E} TL - \frac{4}{y\sigma_{UU} + 1} B \\ &= 4\,B + \frac{3(\sigma_{UU} + 3\sigma_E)y}{\sigma UU(3y\sigma_E - 1)} TB + \frac{4}{3y\sigma_E - 1} B; \end{aligned} \tag{50}$$

$$\begin{aligned} B + L &= -2B - \frac{(\sigma_{UU} + 3\sigma_E)y}{(y\sigma_{UU} + 1)\sigma_E} TL + \frac{4}{y\sigma_{UU} + 1} B, \\ &= -2B - \frac{3(\sigma_{UU} + 3\sigma_E)y}{\sigma_{UU}(3y\sigma_y - 1)} TB - \frac{4}{3y\sigma_E - 1} B \end{aligned} \tag{51}$$

have a more complex form than in the fourth-generation model. Moreover, the coefficients are hyperbolically dependent on the charge parameter. To compensate for such a decrease, one should increase the masses of techniparticles with high charges.

To determine the values of the model parameters for the observed value of the density ratio (i.e., to solve the inverse problem), one should consider the case of the strong suppression of the technibaryonic component of DM ($\frac{\sigma_{UU}}{\sigma_E} \to 0$). Then, the $\frac{L}{B}$ ratio is

$$\frac{L}{B} = \frac{m_{N/E}(y\sigma_{UU} + 1)}{\mp 5.043450334y - m_{N/E}(3y\sigma_{UU} - 1)}, \tag{52}$$

where the sign $\mp$ corresponds to the reverse sign of the charge of the generated excess, and $\frac{\Omega_L}{\Omega_b} = \frac{\Omega_{DM}}{\Omega_b} = \frac{0.265}{0.0493}$. One can see that $\frac{L}{B} \to 1$ because of the high mass of technilepton.

4.2. After the Electroweak Phase Transition

If the temperature of the sphaleron transitions exceeds the temperature of EWPT, the solution of the system of equations has the following form

$$\frac{TB}{B} = -\alpha \left(\frac{L}{B} + \gamma \frac{TL}{B} + \beta \right). \tag{53}$$

Functions

$$\alpha = \frac{\sigma_{UU}}{3}\frac{(\sigma_t+5)(2\sigma_{UU}+\sigma_E)+6(\sigma_t+17)}{(9(\sigma_t-1)y+2(\sigma_t+5))\sigma_{UU}+(\sigma_t+5)\sigma_E+3(5\sigma_t+31)}, \tag{54}$$

$$\beta = \frac{18(2\sigma_{UU}+\sigma_E+18)}{(\sigma_t+5)(2\sigma_{UU}+\sigma_E)+6(\sigma_t+17)}, \tag{55}$$

$$\gamma = \frac{2(\sigma_t+5)\sigma_{UU}+(27(1-\sigma_t)y+\sigma_t+5)\sigma_E+3(5\sigma_t+31)}{\sigma_E((\sigma_t+5)(2\sigma_{UU}+\sigma_E)+6(\sigma_t+17))} \tag{56}$$

look bulky, even in the approximation of equal masses, because of the nonzero mass of t quark. In the limit $m_t \to 0$ or $\sigma_t \to 1$ (which are the same), Equation (53) coincides with the one that was considered in [13,14]:

$$\frac{TB}{B} = \frac{\sigma_{UU}}{3}\left(\frac{L}{B}+\frac{1}{\sigma_E}\frac{TL}{B}+3\right). \tag{57}$$

In Figure 12, coefficients α, β, and γ are plotted as functions of total mass ($m_{UU} = m_{N/E}$). Their behavior is very similar to the reduced version (Equation (57)) but changed by the nonzero mass of t quark. For instance, the function β has the asymptote $\beta = \frac{54}{\sigma_t+17} \approx 3$.

According to Equations (53) and (57), the charge dependence of the density ratio can only be obtained if quark t hA a nonzero mass. Moreover, this dependence is very weak (for $|y| < 100$); so, it cannot play any significant role in the present consideration.

The product of the coefficients $\alpha\gamma$ allows the suppression of the density of technibaryons by using the mass assumption. So, if the difference of masses is high enough, Equation (53) can be rewritten as

$$\frac{\Omega_{DM}}{\Omega_b} \approx -\frac{3m_{N/E}}{m_p}\frac{1}{\gamma}\left(\frac{L}{B}+\beta\right). \tag{58}$$

If $\frac{L}{B} < -\beta \approx -3$, then $y > 0$ should be set to prevent the production of anomalous isotopes. And, similarly, if $\frac{L}{B} > -\beta \approx -3$, then $y < 0$.

In Figure 13, Equation (58) is plotted as a function of total mass in assumption $m_{N/E} = \frac{m_{UU}}{2}$. The ratio $\frac{\Omega_{DM}}{\Omega_b}$ can reach its observed value, but the mass required for this grows when the $\frac{L}{B}$ parameter increases. In Figure 13, the intersection point of the line $\frac{\Omega_{DM}}{\Omega_b} = 5.375$ is shifted to the left in the graph of the $\frac{\Omega_{DM}}{\Omega_b}(m)$ function. So, it is possible to find the upper mass limits. If $\frac{L}{B} < 10^7 - 10^8$ [21], the mass of technileptonic X-helium should be $m_{N/E} < 5 - 8\,\mathrm{TeV}$.

As before, the sign of the density ratio corresponds to the sign of the technilepton number of the excess. In this case, it is determined mainly by the value of the $\frac{L}{B}$ parameter.

In approximation $\sigma_t \to 1$, the sum and difference of the densities of the baryon and lepton numbers have a simple form:

$$B - L = 4\,B + \frac{3}{\sigma_{UU}}\,TB + \frac{1}{\sigma_E}\,TL, \tag{59}$$

$$B + L = -2\,B - \frac{3}{\sigma_{UU}}\,TB - \frac{1}{\sigma_E}\,TL. \tag{60}$$

But, they are very different from those in Equations (50) and (50) obtained in the case where $T > T_c$.

4.3. Discussion

The observed ratio of densities $\frac{\Omega_{DM}}{\Omega_b}$ can be explained using the WTC model. If sphaleron transitions freeze out before the EWPT, the DM should be provided by different forms of

bound states of techniparticles. Technileptonic X-helium can be considered for any value of the charge parameter y, but, when $y < 0$, WIMP-like states arise.

The danger of DM overproduction is the most powerful limiting factor of the model's parameters' values. It gives the low limit on the total mass: $m \geq 1$ TeV. Some regions are forbidden because of the high density of anomalous isotopes. Unfortunately, the upper limits on the masses of particles can be obtained only in particular cases.

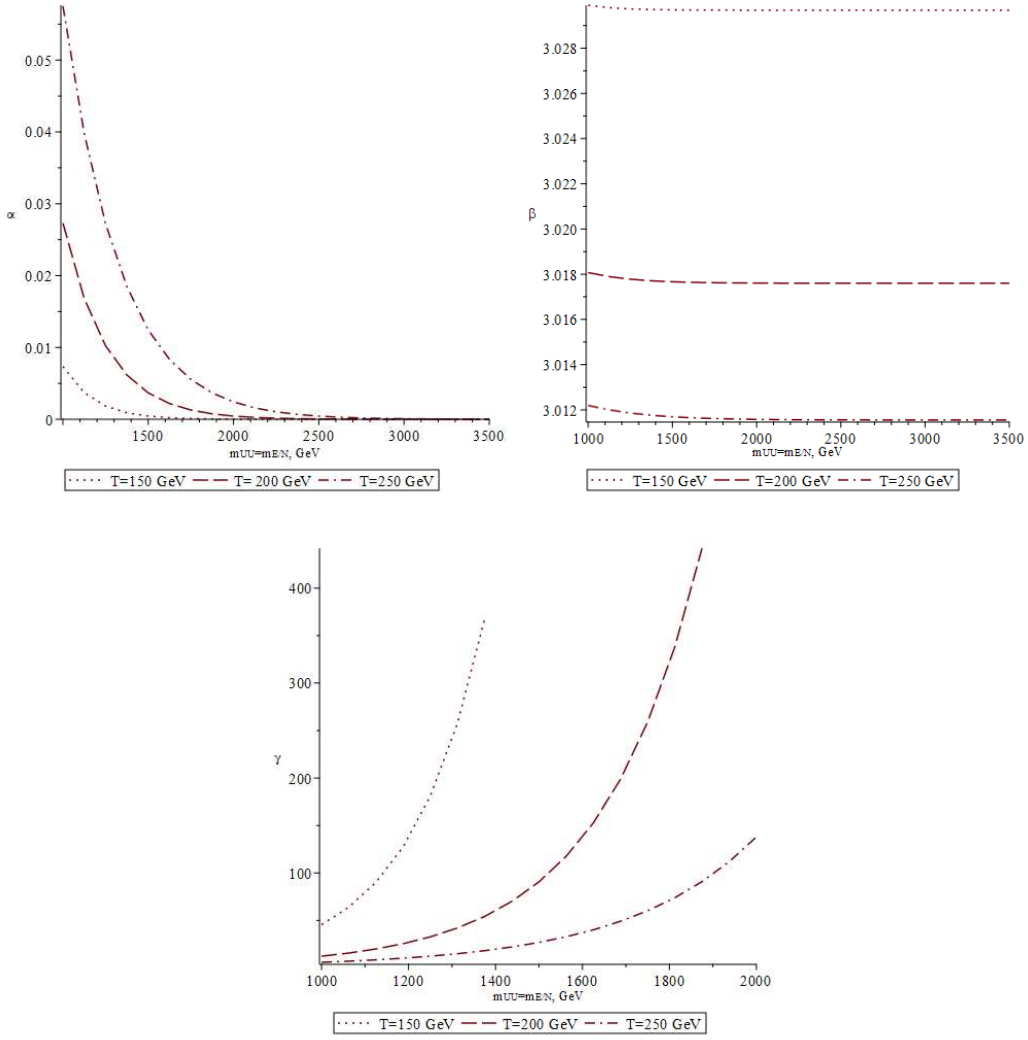

Figure 12. The coefficients of Equation (53) as functions of total mass.

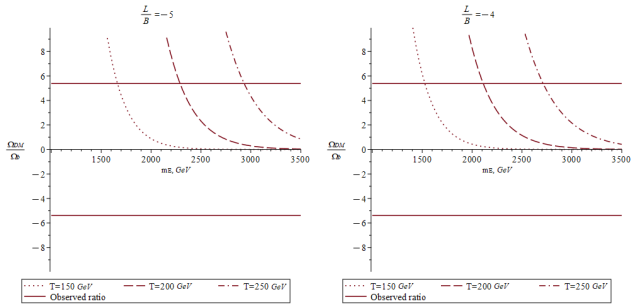

Figure 13. *Cont.*

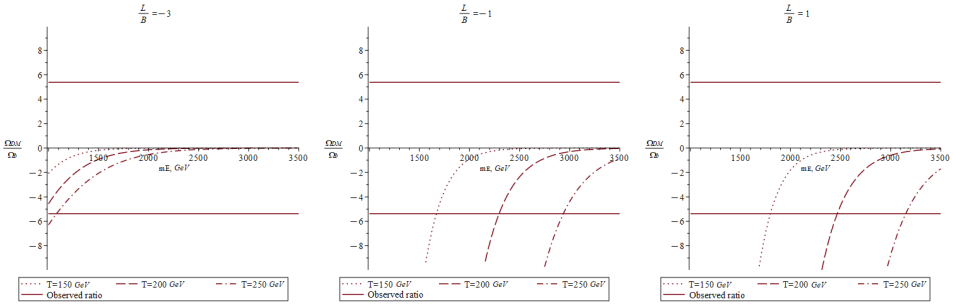

Figure 13. The ratio of densities as a function of total mass for assumption $m_{N/E} = \frac{m_{UU}}{2}$.

The suppression of the technibaryon component allows the simplification of this phenomenology, which indicates the need for a detailed consideration of the effects of the mass difference of new particles on the composition and quantity of DM. The method using the weight function differences proposed in this article can be used to identify the main patterns of density behavior.

This suppression also leads to the low density of WIMPs for most cases. This is consistent with observations.

If sphaleron transitions freeze out after the EWPT, the charge dependence is negligible. In the general case, the limits on masses of new particles cannot be found, but, in the case of a suppressed technibaryonic DM component ($\Omega_{UU} \to 0$), it cannot be too high: $m < 8$ TeV. The removal of suppression should enhance this restriction due to the danger of DM overproduction and/or the formation of WIMP-like bound states.

One also can conclude that the dependence on charge mainly arises due to the additional conditions (like $\mu_0 = 0$ when $T > T_c$). Such conditions should give rise to significant changes in the structure of the DM.

5. The Rate of Sphalerons

The sphaleron rate is, in fact, the normalized probability of the (classical) transition between topologically nonequivalent vacuum states with the closest values of integer Chern–Simons numbers. The process describes an occurrence and the consequent decay of some collective excitation of fields with definite quantum numbers (in particular, baryon and lepton ones). In these transitions, $\Delta(B - L) = 0; \quad \Delta(B + L) \neq 0$. It is assumed that such vacuum transformations for the system of interacted quantum fields can explain the observed baryon asymmetry of the Universe (BAU) using sphaleron connections between lepto- and baryogenesis in a framework of some gauge scheme.

The arise and decay of sphaleron can manifest in multiple-particle production via fluctuations in cosmological plasma at high temperatures (distinct from the quantum tunneling instanton transitions between vacuum states occurring at temperatures close to zero and low energies). The energy of such a multiparticle process strongly depends on the form of the scalar potential at various scales, so the question about the Higgs sector structure and, correspondingly, the gauge symmetry group and content of particles in the model analyzed is of special importance.

Estimations of the sphaleron transition rate per unit time and volume can be derived from classical thermodynamics; in fact, it is the calculation of the high-energy fluctuation probability. Instanton rate calculations have been considered in many papers (for the first and important approaches, see [27,28] and the review [17]). As for sphalerons, there are several ways to quantitatively analyze the sphaleron rate as a function of temperature, including the form of the potential and the dynamics of the quantum fields [17] in SM or some of its extensions (in this study, two of such extensions were considered). The important point is that it is these vacuum–vacuum transitions, described by classical trajectories passing through the maximum of the scalar potential, can provide the correct value of baryon asymmetry due to the connection between baryon and lepton quantum numbers (if Sakharov's conditions are fulfilled).

The observed value of the BAU should be derived from sphaleron parameters (rate, cross-section of production) at various temperatures. These parameters obviously depend on the local characteristics and global behavior of the scalar potential, i.e., on the type and energetic scale of the SM extension. Thus, various modifications of the SM Higgs sector (taking into account triple Higgs interactions or additional Higgs doublets, the emergence of a new scalar field between the epochs of inflation and radiation [29]) or the transition to other scales (from the SM fermions to the forth generation of heavy quarks or to techniquarks and composite scalars) are considered as possible scenarios providing EW baryogenesis due to enhancing sphaleron transitions.

In some papers, BAU generation in the SM framework is (almost) provided due to sphaleron decoupling, i.e., the gradual turning off of sphalerons (depending on their size and rate) from the beginning of the EW phase transition up to sphalerons' freeze-out) [30,31]. Such decoupling of sphalerons generates the necessary degree of disequilibrium in the system, as it is dictated by Sakharov conditions.

Returning to the question of sphaleron rate calculations with purely analytic methods, it is known how to obtain reasonable estimations for the case where the ambient media's temperature is high enough [17,32,33]. Using a quasiclassical approximation for the sphaleron decay width, Γ (note that this approach cannot be used at very low temperatures—where instanton transitions dominate), and when $T \geq E_{sph}$):

$$\Gamma \sim (\frac{m_W^2}{\alpha_W T})^2 \cdot exp(-E_{sph}/T),$$

In this expression, there should be some normalizing factors following from integration over zero modes for sphaleron solutions. Additionally, some additional approximations that underly this quantitative result, particularly important are the two-loop contributions, cannot be considered in this way.

An effective theory [34–37] was suggested that allows us to obtain the sphaleron rate in an analytic way, with a result that is very close to the numerically estimations. At the same time, this approach is formulated in a reasonable physical picture of a baryon number violation in the hot phase. Additionally, it opens the possibility to analyze the sphaleron rate dependence on N_C for general $SU(N_C)$ gauge theory.

A potentially more accurate (or more general) approach involves using Green functions language; as it follows from the calculation of classical correlation function, there is a proportionality between the rate of Yukawa interactions with Higgs fields and the rate of sphaleron transitions with baryon number violation (see [17] and the references within). This connection of the rate of fermion number violation with classical objects—a correlation function—leads, at high temperatures ($T, \quad gT >> m_W(T)$), to the following expression, also from dimensional considerations (here, in the phase with restored symmetry, there is no exponential suppression):

$$\Gamma = (\alpha_W T)^4 F(\frac{\lambda}{g^2}, \frac{m^2(T)}{g^4 T^2}),$$

at very high temperatures for function $F \to 1$.

Note, real-time calculations of baryon number violation processes at high temperatures, which begin from the evolution of classical equations of motion and take into account the initial conditions via their summation with a thermal weight, experience the occurrence of ultraviolet divergences. This means a new scale, ~gT, must be introduced for hard momentum regions to regularize these divergences. In the approach suggested in Refs. [38,39], this can work using an effective Hamiltonian with an ultraviolet cutoff for hard thermal loops. Then, the correct infrared behavior of real-time correlation functions is provided. In fact, this is an approximation of real-time non-erturbative calculations of temperature-dependent sphaleron processes.

Numerically, for the phase with EW-restored symmetry, the rate of sphaleron transitions has the functional form $\Gamma = k \cdot (\alpha_W T)^4$ with factor $k \approx 0.1 - 1.0$. However, the question of the spontaneous CP-breaking value remains open, as does the question of the degree of cosmological plasma nonequilibrium at high energies (i.e., questions about the feasibility of Sakharov's conditions).

The global behavior of scalar potential can manifests via the arising of a second sphaleron branch containing an extra-high-energy state having a half-integer Chern–Simons number with $E_{sph_2} \approx (3-8)E_{sph_1}$. Such an additional sphaleron solution is specific for the minimal composite Higgs model [40] (and the energy of the new-type sphaleron increases linearly with the composite's scale growth). Decreasing sphaleron energy in comparison with the SM can be found in the scenario with deformed potential $V(\phi)$. These specific changes in the sphaleron's energy spectrum [41], resulting from solutions for various types of scalar potential, obviously demonstrate a deep linkage between the quantitative parameters of sphaleron configurations and the complex structure of the nonperurbative vacuum "scene", where this transition takes place.

It seems reasonable to associate the occurrence of the additional sphaleron branches with the manifestations of vacuum characteristics (v.e.v's-like techniquark condensates, for example, which, in principle, can be nonlocal and nonstatic, i.e., some dynamic functions) on a high-energy scale. In other words, the deformation or modification of potential in comparison with the standard model potential, $V(\phi)$, should be a consequence of an effect of some vacuum structures, and can manifest as an additional classic solution of equations of motion at temperature $T \gtrsim m_{sph} \sim < \bar{Q}Q >$; operator $< \bar{Q}Q >$ characterizes the Higgs vacuum averages in the compositeness scenario. For example [42], in the technicolor model, it can be estimated as $\Lambda_{TC} \sim 400 - 500\,\mathrm{GeV}$, $< \bar{Q}Q > \sim \Lambda_{TC}^3$, $v = 246\,\mathrm{GeV}$.

The nonperturbative nature of sphaleron processes indicates the obvious effectiveness of lattice calculation methods for the sphaleron rates. In Ref. [17], some first estimations of prefactors (summing zero modes for vacuum-vacuum transitions) for known temperature dependences of the rates in the symmetric and broken phases are given. Then, lattice studies of the sphaleron rates for different temperature ranges in pure-gauge $SU(2)$, pure-glue strong theory, symmetric phase, and broken phase have evolved and been improved significantly using different approaches [43–46]. So, to date, there are known calculated values both for the temperature dependence of Higgs field vacuum condensate and for prefactors that sum the nonperturbative small fluctuations against the background of the sphaleron solution.

Particularly, the temperature dependence of the vacuum average for Higgs field $v(T)$ was calculated for a sharp EW crossover at $T_c \approx 159\,\mathrm{GeV}$ in the symmetric phase $\Gamma_{sph}/T^4 \approx (18 \pm 3)\alpha_W^5$, which is almost constant, but, in the broken phase, $140\,\mathrm{GeV} \leq T \leq 155\,\mathrm{GeV}$, a stable approximation was found: $\ln \Gamma / T^4 = (0.83 \pm 0.01)T - (147 \pm 1.9)$ [44]. Moreover, from the lattice consideration, a reasonable estimation of the freeze-out temperature was found in the early Universe (defined as the temperature of cosmological plasma when the Hubble rate exceeds the rate of the baryon number violation): $T_* = (131.7 \pm 2.3)\,\mathrm{GeV}$. In principle, this set of model parameters provides low-scale leptogenesis scenarios.

Lattice methods were applied to QCD sphalerons, and, in the pure-gauge case where $T \approx 1.24 T_c$, where $T - C \approx 300\,\mathrm{MeV}$, it was found that $\Gamma_{sph} = 0.079(25) \cdot T^4$ in the symmetric phase [45].

Additionally, the calculation of the sphaleron transition in (2 + 1) QCDs was also realized for various temperatures [46]. A comparison of the lattice results for sphaleron rates that have been found by different groups and based on different approaches demonstrates a good agreement between calculations when the same region of temperatures in the framework of the same gauge scheme are considered. So, some impressive convergence of numerical estimations of sphaleron rates in different phases can be seen, and these calculations provide the possibility of formulating some suggestions for experimental sphaleron observation. Certainly, it again returns us to the necessity of conducting detailed

behaviour analysis of the sphaleron production cross-section at various temperatures and phases and studying the sphaleron energy spectrum using various models.

Note, the lattice simulations were used also in the new region of study of the rate of baryon number violation (the sphaleron rate) in SM with an external magnetic field [30,47] for temperatures in the vicinity of crossover, mostly in the broken phase. The emergence of strong magnetic fields and their impact on cosmological plasma fluctuations near the phase transition point represent very significant phenomena in the early stages. It was indicated that quark-gluon plasma has a strong magnetic field that is produced by the hard interactions of heavy ions. Due to sphaleron transitions, local fluctuations and imbalance in left- and right-handed quark densities are produced in plasma, which create the so-called chiral magnetic effect, which results in an electric current that is parallel to the magnetic field. Studying hot plasma with these new electromagnetic properties is a new field for lattice methods. The temperature dependence of the Higgs vacuum average, the value of the critical temperature, and its shift to lower values with increasing external magnetic field (characteristics of hot plasma) can be computed with the lattice approach very effectively [48].

Thus, modifications of the scalar sector lead to noticeable changes in the sphaleron energy. In SM modifications with deformed Higgs potential [41], the sphaleron energy decreases in comparison with that of the standard $V(\phi)$. In the extended Higgs sector [49,50] with a triple Higgs vertex, significant changes in E_{sph} arise due to λ_3 coupling, namely, $\Delta E_{sph} \sim -\lambda_3$. It can be concluded that the measured (in some way) sphaleron energy should contain information on the type of scalar sector.

Already, there are suggestions on how to extract information about sphaleron production and decay from collider or astrophysical data [15,16,51–54]. Indeed, in the search for sphaleron manifestations with the LHC, IceCube, or LHAASO, for the quantitative analysis of hard inelastic scattering of neutrino or other very-high-energy cosmic-ray particles, and for the interpretation of specific and typical sphaleron multiparticle events observed using space telescopes and induced by cosmic particles, reliable estimations of the sphaleron rates and cross-sections are necessary. And, extension of the SM gauge symmetry can be used to provide a correct picture of baryogenesis that is in agreement with the observed BAU value. For consideration of such phenomena in a wide interval of temperatures, various types of modified scalar potentials and models beyond the standard model can be analyzed. Here, the possibilities of simultaneously considering DM and BAU (unstable sphalerons providing a linkage between lepto- and baryogenesis, i.e., baryon asymmetry) in two different scenarios for the SM extension were studied.

Additionally, an important new perspective on the vacuum structure that determines energy, rate, and/or sphaleron cross-section has been suggested in Refs. [53,55,56]. Namely, a periodicity of the scalar potential [53,56] along the axis of Chern-Simons vacuum numbers allows us to obtain an equation of motion of the Schroedinger type and to solve it, resulting in a wave function (of the Bloch type from solid-state physics). The wave function can be used to calculate the probability of the transition between different vacua states, i.e., the sphaleron rates. In fact, this approach claims that this transition should be unsuppressed in the broken phase for energies above E_{sph}, in contradiction with the predicted exponential damping in this region. Certainly, this new picture is optimistic for programming the experimental search of sphaleron events. It should be, however, noted that the specific property of the potential in vacuum space resulting in resonance amplification of the rate for the transition between neighboring minima was reanalyzed [57]. It is noted that some time dependence was missed in the periodic approach, and consideration of the transitions between coherent states in the WKB approximation demonstrates the conservation of exponential suppression for $B + L$-changing processes. This is an opposite, pessimistic prediction for the experimental study of sphalerons in high-energy processes. In any case, the problem of the reliability of the sphaleron rate and cross-section calculations has not been solved completely.

It was found recently that the rate of strong sphalerons is important for axion physics, their production, and their interactions at early stages [58]. Because axions can be used to explain the nature and features of DM, it is important to know the key processes and parameters that can affect axion interactions with each other and with the matter. An emergence in the high-energy plasma system of the strong QCD sphaleron transitions, as it was shown, can significantly change the rates of axion creation and annihilation, i.e., the density of these super-light DM candidates should depend on the rate of vacuum transitions governed by the strong dynamics in hot plasma.

For scenarios with additional heavy fermionic degrees of freedom (like those that were considered above: the fourth generation with new fermions or WTC with heavy techniquarks), an important question was studied: how does the presence of nonstandard heavy fermions change the parameters of the vacuum–vacuum transition? More exactly, how does the energy for the minimal path between topologically distinct vacua deform due to presence of additional fermions [59–61]? A strong deformation of the sphaleron barrier was found in the case of heavy doublet fermions with $m_F \sim$ TeV (the barrier energy decreases significantly with the growth in fermion mass), and an extra fermion branch emerges if $m_F \sim 10\,\text{TeV}$. Moreover, at the top of the barrier, the sphaleron configuration does not show reflection symmetry because of interactions with fermions. Then, the Chern–Simons number for sphaleron is $n_{CS} \neq 1/2$ exactly.

The influence of the fermion Dirac sea on the minimal energy path between neighboring vacuum states in EW theory results in the suppression of the transition rate; the quantum correction of the classical sphaleron energy was also calculated. Thus, the presence of a fermion sea noticeably affects the sphaleron barrier and speed at nonzero temperatures.

6. Conclusions

From the consideration of two scenarios with additional heavy fermions, we found that the observed value of the $\frac{\Omega_{DM}}{\Omega_b}$ ratio can be reasonably explained in both cases. In both models, as shown in our results, the value of the $\frac{L}{B}$ parameter must be quite small.

The rate of sphaleron transition strongly depends on the temperature, so it seems that an excess of DM particles compared with baryons has a fixed value in the early Universe. At the same time, sphaleron transition is a rare process under modern conditions, and it is unlikely to be detected at the moment. Unambiguously distinguishing the necessary events from the background of various multiparticle final states is a hard experimental problem.

In any case, the presented and discussed calculations not only give some guidance regarding the detection of new particles with masses $m \sim$ 1–10 TeV for ground-based colliders or cosmic-ray observatories but also increase our understanding of how the complex structure of A nonperturbative vacuum can manifest within the existence of classic unstable solutions. Studying and possibly observing vacuum–vacuum transitions with baryon number violations in high-energy events could not only prove the predictions of nonperturbative electroweak theory but also give a key to the physics beyond the SM.

Author Contributions: Conceptualization, M.Y.K.; formal analysis, D.O.S. and V.A.B.; writing—original draft preparation, D.O.S. and V.A.B.; writing—review and editing, M.Y.K. All authors have read and agreed to the published version of the manuscript.

Funding: The research by M.Y.K. was carried out at the Southern Federal University with the financial support of the Ministry of Science and Higher Education of the Russian Federation (state contract GZ0110/23-10-IF). The research by D.O.S. was performed within the framework of MEPHI program on Prioritet 2030.

Data Availability Statement: No new data were created or analyzed in this study.

Conflicts of Interest: The authors declare no conflict of interest.

References

1. Beylin, V.; Khlopov, M.; Kuksa, V.; Volchanskiy, N. New Physics of Strong Interaction and Dark Universe. *Universe* **2020**, *6*, 196. [CrossRef]
2. Feng, J.L. Dark Matter Candidates from Particle Physics and Methods of Detection. *Annu. Rev. Astron. Astr.* **2010**, *48*, 495–545. [CrossRef]
3. Belotsky, K.; Khlopov, M.; Shibaev, K. Stable quarks of the 4th family? *arXiv* **2008**, arXiv:0806.1067.
4. Golubkov, Y.; Konoplich, R.; Mignani, R.; Fargion, D.; Khlopov, M. Possible manifestations of the existence of a fourth-generation neutrino. *J. Exp. Theor. Phys.* **1999**, *69*, 402–406. [CrossRef]
5. Beylin, V.; Khlopov, M.; Sopin, D. Charge Asymmetry of New Stable Families in Baryon Asymmetrical Universe. *Symmetry* **2023**, *15*, 657. [CrossRef]
6. Maltoni, M.; Novikov, V.A.; Okun, L.B.; Rozanov, A.N.; Vysotsky, M.I. Extra quark-lepton generations and precision measurements. *Phys. Lett. B* **2000**, *476*, 107–115. [CrossRef]
7. Khlopov, M. New symmetries in microphysics, new stable forms of matter around us. *arXiv* **2006**, arXiv:astro-ph/0607048.
8. Sannino, F.; Tuominen, K. Orienfold Theory Dynamics and Symmetry Breaking. *Phys. Rev. D* **2005**, *71*, 051901. [CrossRef]
9. Hong, D.K.; Hsu, S.D.; Sannino, F. Composite Higgs from higher representations. *Phys. Lett. B* **2004**, *597*, 89–93. [CrossRef]
10. Dietrich, D.D.; Sannino, F.; Tuominen, K. Light composite Higgs from higher representations versus electroweak precision measurements. Predictions for LHC. *Phys. Rev. D* **2005**, *72*, 055001. [CrossRef]
11. Dietrich, D.D.; Sannino, F.; Tuominen, K. Light composite Higgs and precision electroweak measurements on the Z resonance: An update. *Phys. Rev. D* **2006**, *73*, 037701. [CrossRef]
12. Gudnason, S.B.; Kouvaris, C.; Sannino, F. Dark matter from new technicolor theories. *Phys. Rev. D* **2006**, *74*, 095008. [CrossRef]
13. Khlopov, M.Y.; Kouvaris, C. Composite dark matter from a model with composite Higgs boson. *Phys. Rev. D* **2008**, *78*, 065040. [CrossRef]
14. Khlopov, M.Y.; Kouvaris, C. Strong interactive massive particles from a strong coupled theory. *Phys. Rev. D* **2008**, *77*, 065002. [CrossRef]
15. Brooijmans, G.; Schichtel, P.; Spannowsky, M. Cosmic ray air showers from sphalerons. *Phys. Lett. B* **2010**, *16*, 213–218. [CrossRef]
16. Ellis, J.; Sakurai, K.; Spannowski, M. Search for sphalerons: IceCube vs. LHC. *J. High Energy Phys.* **2016**, *2016*, 85. [CrossRef]
17. Rubakov, V.A.; Shaposhnikov, M.E. Electroweak baryon number non-conservation in the early Universe and in high-energy collisions. *Phys. Usp.* **1996**, *39*, 461. [CrossRef]
18. Harvey, A.J.; Turner, M.S. Cosmological baryon and lepton number in the presence of electroweak fermion-number violation. *Phys. Rev. D* **1990**, *42*, 3344–3349. [CrossRef]
19. Kuzmin, V.; Shaposhnikov, M.; Rubakov, V. On the Anomalous Electroweak Baryon Number Nonconservation in the Early Universe. *Phys. Rev. B* **1985**, *155*, 36–42.
20. The Planck Collaboration. Planck 2018 results. VI. Cosmological parameters. *Astron. Astrophys* **2020**, *641*, A6. [CrossRef]
21. Domcke, V.; Kamada, K.; Mukaida, K.; Schmitz, K.; Yamada, M. New Constraint on Primordial Lepton Flavor Asymmetries. *Phys. Rev. Lett.* **2023**, *130*, 261803 [CrossRef]
22. The ATLAS Collaboration. Search for heavy long-lived charged R-hadrons with the ATLAS detector in $3.2 fb^{-1}$ of proton–proton collision data at $\sqrt{s} = 13$ TeV. *Phys. Lett. B* **2016**, *760*, 647. [CrossRef]
23. Canepa, A. Searches for supersymmetry at the Large Hadron Collider. *Rev. Phys.* **2019**, *4*, 100033. [CrossRef]
24. Lee, L.; Ohm, C.; Soffer, A.; Tien-Tien, Y. Collider Searches for Long-Lived Particles Beyond the Standard Model. *Prog. Part. Nucl. Phys.* **2019**, *106*, 210–255. [CrossRef]
25. The ATLAS Collaboration. Search for heavy long-lived multi-charged particles in the full LHC Run 2 pp collision data at $\sqrt{s}$ = 13 TeV using the ATLAS detector. *arXiv* **2023**, arXiv:2023.13613.
26. Khlopov, M. What comes after the Standard Model? *Prog. Part. Nucl. Phys.* **2020**, *116*, 103824. [CrossRef]
27. Son, D.T.; Rubakov, V.A. Instanton-like Transitions at High Energies in (1 + 1) Dimensional Scalar Models. *Nucl. Phys. B* **1994**, *422*, 195. [CrossRef]
28. Son, D.T.; Rubakov, V.A.; Tinyakov, P.G. Classical boundary value problem for instanton transitions at high energies. *Phys. Lett. B* **1992**, *287*, 342.
29. Loc, N.P.D. Sphaleron bound in some nonstandard cosmology scenarios. *Int. J. Mod. Phys. A* **2022**, *37*, 2250153. [CrossRef]
30. Kharzeev, D.; Shuryak, E.; Zahed, I. Sphalerons, baryogenesis, and helical magnetogenesis in the electroweak transition of the minimal standard model. *Phys. Rev. D* **2020**, *102*, 073003. [CrossRef]
31. Hong, M.; Kamada, K.; Yokoyama, J. Baryogenesis from sphaleron decoupling. *arXiv* **2023**, arXiv:2304.13999.
32. Arnold, P.; McLerran, L. Sphalerons, small Suctuations, and baryon-number violation in electroweak theory. *Phys. Rev. D* **1987**, *36*, 2. [CrossRef] [PubMed]
33. Arnold, P.B.; Son, T.D.; Yaffe, L.G. The Hot baryon violation rate is $\sim \alpha_w^5 \cdot T^4$. *Phys. Rev. D* **1997**, *55*, 6264. [CrossRef]
34. Bodeker, D. Effective dynamics of soft non-abelian gauge fields at finite temperature. *Phys. Lett. B* **1998**, *426*, 351. [CrossRef]
35. Bodeker, D. Diagrammatic approach to soft non-Abelian dynamics at high temperature. *Nucl. Phys. B* **2000**, *566*, 402. [CrossRef]
36. Bodeker, D.; Buchmuller, W. Baryogenesis from the weak scale to the grand unification scale. *Rev. Mod. Phys.* **2021**, *93*, 035004. [CrossRef]
37. Moore, G.D. Do We Understand the Sphaleron Rate? *arXiv* **2000**, arXiv:hep-ph/0009161.

38. Ambjørn, T.; Askgaard, H.; Porter, H.; Shaposhnikov, M. Sphaleron transitions and baryon asymmetry: A numerical, real-time analysis. *Nucl. Phys. B* **1991**, *383*, 346. [CrossRef]
39. Bodeker, D.; McLerran, L.; Smilga, A. Really Computing Non-perturbative Real Time Correlation Functions. *Phys. Rev. D* **1995**, *52*, 4675. [CrossRef]
40. Agashe, K.; Contino, R.; Pomarol, A. The Minimal Composite Higgs Model. *Nucl. Phys. B* **2005**, *719*, 165. [CrossRef]
41. Spannowsky, M.; Tamarit, C. Sphalerons in composite and nonstandard Higgs models. *Phys. Rev. D* **2017**, *95*, 015006. [CrossRef]
42. Hill, C.T.; Simmons, E.H. Strong dynamics and electroweak symmetry breaking. *Phys.Rept.* **2003**, *381*, 402. [CrossRef]
43. D'Onofrio, M.; Rummukainen, K.; Tanberg, A. The sphaleron rate at the electroweak crossover with 125 GeV Higgs mass. In Proceedings of the PoS: The 30th International Symposium on Lattice Field Theory, (Lattice 212), Cairns , Australia, 24–29 June 2012.
44. D'Onofrio, M.; Rummukainen, K.; Tanberg, A. The Sphaleron Rate in the Minimal Standard Model. *Phys. Rev. Lett.* **2014**, *113*, 141602. [CrossRef] [PubMed]
45. Barroso Mancha, M.; Moore, G.D. The sphaleron rate from 4D Euclidean lattices. *J. High Energy Phys.* **2023**, *01*, 155. [CrossRef]
46. Bonanno, C.; D'Angelo, F.; D'Elia, M.; Maio, L.; Naviglio, M. Sphaleron rate as an inverse problem: A novel lattice approach. In Proceedings of the PoS: The 40th International Symposium on Lattice Field Theory, (Lattice 2023), Batavia, IL, USA, 31 July–4 August 2023.
47. Vachaspati, T. Progress on cosmological magnetic fields. *Rep. Prog. Phys.* **2021**, *84*, 074901. [CrossRef]
48. Annala, J.; Rummukainen, K. Electroweak sphaleron in a magnetic field. *Phys. Rev. D* **2023**, *107*, 073006. [CrossRef]
49. Kanemura, S.; Tanaka, M. Higgs boson coupling as a probe of the sphaleron property. *Phys. Lett. B.* **2020**, *809*, 135711. [CrossRef]
50. Hu, J.Y.; Zhou, S. Sphalerons in the Higgs triplet model. *J. High Energy Phys.* **2023**, *10*, 004. [CrossRef]
51. Bezrukov, F.; Levkov, D.; Rebbi, C.; Rubakov, V.; Tinyakov, P. Semiclassical Study of Baryon and Lepton Number Violation in High-Energy Electroweak Collisions. *Phys. Rev. D* **2003**, *68*, 036005. [CrossRef]
52. Ellis, J.; Sakurai, K. Search for sphalerons in proton-proton collisions. *J. High Energy Phys.* **2016**, *2016*, 86. [CrossRef]
53. Tye, S.-H.H.; Wong, S.C.S. Baryon number violating scatterings in laboratories. *Phys. Rev. D* **2017**, *96*, 093004. [CrossRef]
54. Jaeckel, J.; Yin, W. High Energy Sphalerons for Baryogenesis at Low Temperatures. *Phys. Rev. D* **2023**, *107*, 015001. [CrossRef]
55. Qiu, Y-C.; Tye, S.-H.H. Role of Bloch waves in baryon-number violating processes. *Phys. Rev. D* **2019**, *100*, 033006. [CrossRef]
56. Tye, S.-H.H.; Wong, S.C.S. Bloch wave function for the periodic sphaleron potential and unsuppressed baryon and lepton number violating processes. *Phys. Rev. D* **2015**, *92*, 045005. [CrossRef]
57. Funakubo, K.; Fuyuto, K.; Senaha, E. Does a band structure affect sphaleron processes? *arXiv* **2016** , arXiv:1612.05431.
58. Notari, A.; Rompineve, F.; Villadoro, G. Improved Hot Dark Matter Bound on the QCD Axion. *Phys. Rev. Lett.* **2023**, *131*, 011004. [CrossRef] [PubMed]
59. Nolte, G.; Kunz, J. The sphaleron barrier in the presence of fermions. *Phys. Rev. D* **1993**, *48*, 5905. [CrossRef] [PubMed]
60. Diakonov, D.; Polyakov, M.; Sieber, P.; Schaldach, J.; Goeke, K. Fermion Sea Along the Sphaleron Barrier. *Phys. Rev. D* **1994**, *49*, 6864. [CrossRef] [PubMed]
61. Petriashvili, G. Electroweak non-topological solitons and baryon number violation in the standard model. *Nucl. Phys. B* **1992**, *378*, 468–486. [CrossRef]